LEARNING A DENSE REASONING REWARD MODEL FROM EXPERT DEMONSTRATION VIA INVERSE REINFORCEMENT LEARNING

Anonymous authors
Paper under double-blind review

ABSTRACT

We reframe and operationalise adversarial inverse reinforcement learning (IRL) to large language model reasoning, learning a dense, token-level reward model for process supervision directly from expert demonstrations rather than imitating style via supervised fine-tuning. The learned reasoning reward serves two complementary roles: (i) it provides step-level feedback to optimise a reasoning policy during training; and (ii) it functions at inference as a critic to rerank sampled traces under fixed compute budgets. We demonstrate that our approach prioritises correctness over surface form, yielding scores that correlate with eventual answer validity and enabling interpretable localisation of errors within a trace. Empirically, on GSM8K and MedReason with Llama3 and Qwen2.5 backbones, we demonstrate: (i) dense reasoning rewards can be used as a learning signal to elicit reasoning, and (ii) predictive performance is improved from reward-guided reranking (notably for Llama-based policies). By unifying training signals, inference-time selection, and token-level diagnostics into a single reasoning reward, this work suggests reusable process-level rewards with broad potential to enhance multi-step reasoning in language models.[1]

1 INTRODUCTION

Recent advancements in large language models (LLMs) have driven rapid progress on multi-step reasoning tasks. A dominant method is to transfer reasoning behaviours from human experts or stronger models via supervised fine-tuning (SFT) on their reasoning traces (DeepSeek-AI et al., 2025). While effective, this strategy fundamentally trains models to imitate a teacher's style, rather than to optimise reasoning as a decision-making process. Moreover, pure imitation omits the exploration–exploitation trade-off that underpins autonomous improvement in sequential decision-making (Setlur et al., 2025).

We take a different route: we formulate process-level reasoning as an inverse reinforcement learning (IRL) problem. Instead of behaviour cloning from teacher LLMs (Sun and Schaar, 2025), we learn a dense reasoning reward model from expert demonstrations. This reasoning reward model evaluates intermediate steps within a reasoning trace and supplies token-wise feedback used in two complementary ways: (i) as a training signal to optimise a policy for reasoning, and (ii) at inference time, as an assistive reranker to select higher-quality samples under a fixed budget. In contrast to behaviour cloning, this IRL-based approach aims to encode principles of expert reasoning and to expose where a trace deviates from a good path through interpretable, dense rewards.

Defining a faithful, scalable, dense reward for reasoning is non-trivial: hand-crafted signals are task-specific, and often incentivise shortcuts. By contrast, expert reasoning traces are comparatively easier to collect at scale than carefully engineered token-level reward functions, and they implicitly contain information about which intermediate steps matter. We therefore learn the dense reward from expert demonstrations, rather than prescribing it, and use it for both training and inference-time assistance.

[1]We provide the code for our experiments at https://anonymous.4open.science/r/expert_reasoning-C1E8

We centre our formulation around four desiderata, evaluated empirically in this work:

1. **(D1) A reward model usable to train reasoning in an LLM.** Training with only outcome correctness lacks step-level guidance and encourages shortcut learning. Our learned reasoning reward model provides dense, token-level rewards that serve as a training signal for policy optimisation.
2. **(D2) An inference-time assist to improve predictive performance.** In deployment, we often have a small sampling budget; reranking or filtering can yield significant gains without retraining. We use the reasoning reward model to score and rerank sampled traces under a fixed budget.
3. **(D3) Reward prefers being more likely correct, not only matching expert style.** Style imitation can embed biases and does not guarantee correctness. We show that the reasoning reward scores correlate positively with eventual correctness, rather than just surface form.
4. **(D4) Interpretable dense reward that localises errors.** Process supervision should enable auditing and targeted intervention. We demonstrate how our reasoning reward model highlights erroneous steps within a trace, exposing where and how the reasoning deviates from the correct course.

We explicitly separate capability from predictive performance supremacy. Jointly optimising a policy with a learned process reward model realises the four desiderata above: (D1) a usable training signal, (D2) inference-time gains via reward-guided reranking under tight sampling budgets, (D3) rewards that favour likely-correct traces over mere stylistic conformity, and (D4) token-level diagnostics. Our main results centre on these capabilities—showing dense, token-level supervision, improved predictive performance via reward-guided selection, and interpretable error localisation.

A systematic overview of our method to learn a dense reasoning reward model is shown in Figure 1.

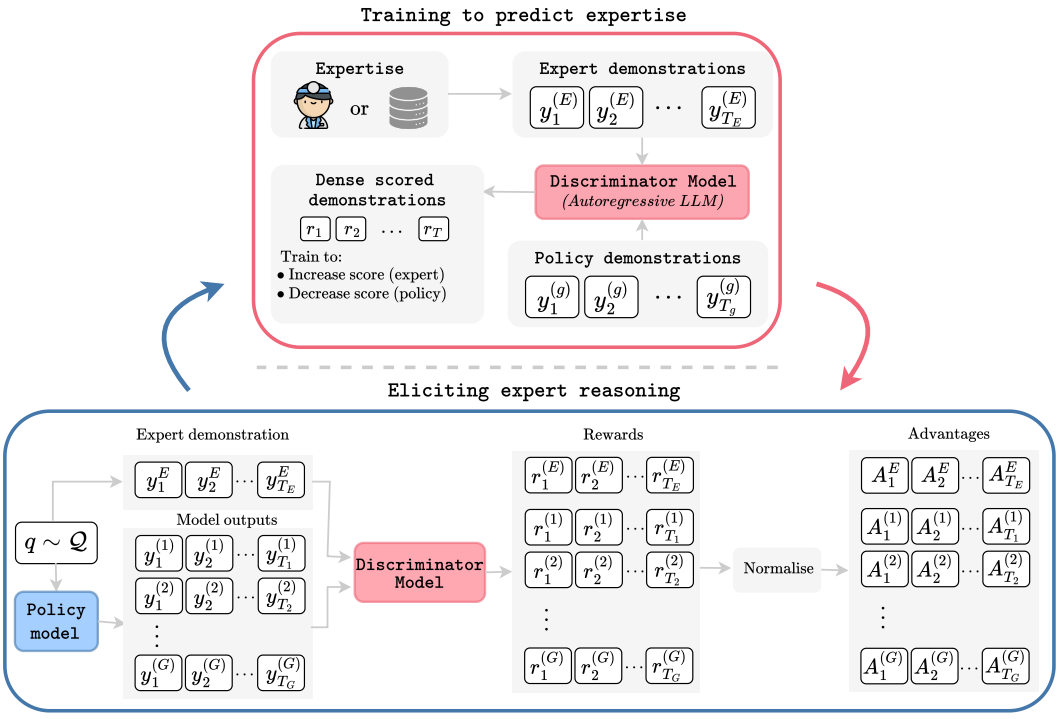

Figure 1: **Eliciting expert reasoning via adversarial inverse reinforcement learning**. The model learns a reasoning reward function from expert demonstrations using adversarial IRL.

2 Related Work

Reinforcement Learning and Search for Reasoning. There is growing interest in using reinforcement learning (RL) to equip language models with improved reasoning by framing it as a sequential decision-making problem. Process supervision leverages process reward models (PRMs) to score intermediate steps rather than only final answers (DeepSeek-AI et al., 2025). This has been used to guide models in maths and logic by rewarding stepwise correctness (Uesato et al., 2022; Lightman et al., 2023), encouraging human-like solution paths in principle. However, specifying faithful, fine-grained rewards is non-trivial, and training separate PRMs invites reward hacking and additional complexity. Search-based approaches such as Monte Carlo Tree Search (MCTS) explore multiple reasoning paths and assign credit to steps that culminate in correct solutions (Zelikman et al., 2022; Yuan et al., 2023; Singh et al., 2024; Hosseini et al., 2024), echoing successes in games (Silver et al., 2017). Yet scaling MCTS to language is difficult due to the vast branching factor and noisy valuation of partial solutions. Closer to our aims, Cui et al. (2025) seeks to learn dense reasoning rewards via implicit rewards (Rafailov et al., 2024) and outcome-verifiable signals. Our work differs in that we learn a dense, token-level reward from expert demonstrations and utilise it both as a training signal and as an inference-time reranker.

Inverse Reinforcement Learning for LLM Alignment. Inverse reinforcement learning (IRL) infers a reward function from demonstrations rather than assuming it is known (Ziebart et al., 2004; Abbeel and Ng, 2004; Hejna and Sadigh, 2023; Fu et al., 2019; Ho and Ermon, 2016). This is attractive for aligning LLMs with human preferences and complex reasoning objectives that are difficult to specify, such as those used in RL with human feedback (RLHF) with preference data (Christiano et al., 2023; Rafailov et al., 2024). Recent works formalise alignment for language models as sequential decision-making with missing rewards (Sun and van der Schaar, 2024; Xia et al., 2024; Sun and van der Schaar, 2025), inferring rewards from high-quality trajectories (human experts or reliable AIs) to guide behaviour (Joselowitz et al., 2024).In traditional IRL literature, adversarial IRL methods train a discriminator to separate expert from generated traces and convert it into a reward (Ho and Ermon, 2016; Fu et al., 2018; Lin and Zhang, 2018; Li et al., 2017). We take this adversarial IRL perspective to learn a dense process-level critic from expert reasoning traces. This directly supports (D1) by providing a usable training signal, (D2) via inference-time reranking using the same critic, (D3) by favouring likely-correct traces rather than stylistic conformity, and (D4) by yielding token-level diagnostics.

Distillation and Supervised Fine-Tuning of Reasoning. A direct path to training reasoning models is supervised learning on demonstrations or rationales, often framed as knowledge distillation (Hinton et al., 2015). High-quality traces, from humans or strong teacher models, can be imitated to improve reasoning (DeepSeek-AI et al., 2025; Kang et al., 2023; Kujanpää et al., 2025; Xu et al., 2025). While SFT with chain-of-thought improves performance without RL's optimisation challenges, pure imitation cannot explore or correct out-of-distribution states (Setlur et al., 2025). In our evaluation, SFT serves as a strong baseline for predictive performance. In contrast, our IRL-based approach prioritises capabilities: a reusable dense reward for training (D1), inference-time gains via reranking (D2), correctness-oriented scoring (D3), and interpretable token-level diagnostics (D4).

We summarise methodological differences with an emphasis on our desiderata in Table 1. The comparison highlights which approaches (i) learn a reward, (ii) provide dense, step-level signals, (iii) use expert demonstrations, (iv) naturally support inference-time assist (reranking/selection), and (v) generalise beyond stylistic imitation.

3 Problem Formalism

We model reasoning as an autoregressive, sequential decision-making process. Given a prompt x, at step t the system is in state $s_t = (x, y_{<t})$ with $y_{<t} = (y_1, \ldots, y_{t-1})$. The action space coincides with the vocabulary $\mathcal{V}$; an action is the next token $y_t \in \mathcal{V}$. An output (reasoning trace) is a trajectory $\tau = (y_{1:T})$ of length T. The LLM, parameterised by θ, induces a policy

$$\pi_\theta(a_t \mid s_t) = \pi_\theta(y_t \mid x, y_{<t}),$$

and thereby a trajectory distribution $p_\theta(\tau \mid x)$ over $\mathcal{T}$, the space of token sequences. We write $x \sim \mathcal{Q}$ for the prompt distribution and $\tau_\theta \sim p_\theta(\cdot \mid x)$ for trajectories sampled from the current policy.

Method	Examples	Optimisation Objective	Learned Reward	Dense	Uses Experts	Inference Assist	Generalise beyond Style
SFT	DeepSeek-AI et al. (2025) Setlur et al. (2025) Kang et al. (2023)	$\max_\theta \mathbb{E}_{(x,y)\sim\mathcal{D}} [-\sum_t \log p_\theta(y_t \mid x, y_{<t})]$	✗	✗	✓	✗	✗
Outcome Sup.	DeepSeek-AI et al. (2025)	$\max_\theta \mathbb{E}_{\tau\sim\pi_\theta} [\, r_{\text{out}}(\tau)\,]$	✗	✗	✗	✓	✓
Process-Sup.	Uesato et al. (2022) Lightman et al. (2023) Singh et al. (2024) Hosseini et al. (2024)	$\max_\theta \mathbb{E}_{\tau\sim\pi_\theta} \left[\sum_t r_{\text{proc}}(y_t)\right]$	✗	✓	✗	✓	✓
RLHF	Christiano et al. (2023)	$\max_\theta \mathbb{E}_{\tau\sim\pi_\theta} \left[\sum_t r_\phi(y_t)\right]$	✓	(✗)	(✓)	✓	✓
Expert Reas.	**ours**	$\max_\phi \min_\theta (\mathbb{E}_{\tau_E\sim p_E}[r_\phi(\tau_E)] - \mathbb{E}_{\tau_\theta\sim p_\theta}[r_\phi(\tau_\theta)])$	✓	✓	✓	✓	✓

Table 1: **Comparison against desiderata.** Columns indicate whether a method (i) learns a reward, (ii) provides dense step-level signals (D1/D4), (iii) leverages expert demonstrations, (iv) naturally supports inference-time assistance via scoring/reranking (D2), and (v) facilitates generalisation beyond stylistic imitation towards correctness (D3).

Our goal is to learn π_θ that generates trajectories exhibiting high-quality chain-of-thought reasoning before answering. Unlike classical RL, an explicit reward is not observed: the latent evaluation function $r : \mathcal{T} \to \mathbb{R}$ (or token-level $r : \mathcal{S} \times \mathcal{V} \to \mathbb{R}$) is unknown. Instead, we assume access to expert demonstrations $\mathcal{D}_E = \{\tau_i^E\}_{i=1}^N$ drawn from an expert distribution $p_E(\tau \mid x)$, where each τ_i^E is a high-quality reasoning trace produced by a human expert or a stronger teacher model. The learning problem is to use $\mathcal{D}_E$ to infer the structure of effective reasoning and to optimise π_θ so that $p_\theta(\cdot \mid x)$ aligns with $p_E(\cdot \mid x)$ while solving the underlying tasks.

To bridge to our IRL formulation, we introduce a parametric surrogate reward $r_\phi : \mathcal{T} \to \mathbb{R}$. The generic adversarial IRL objective seeks a saddle point in which the reward parameters ϕ maximise the separation between expert and policy trajectories while the policy parameters θ minimise it:

$$\max_\phi \min_\theta \mathbb{E}_{x\sim\mathcal{Q}}\Big[\mathbb{E}_{\tau_E\sim p_E(\cdot|x)}\big[r_\phi(\tau_E)\big] - \mathbb{E}_{\tau_\theta\sim p_\theta(\cdot|x)}\big[r_\phi(\tau_\theta)\big]\Big]. \tag{1}$$

This objective formalises the goal: learn r_ϕ that scores expert reasoning higher than policy reasoning, while updating π_θ to close this gap.

4 Method

We build on adversarial learning frameworks for inverse reinforcement learning (Fu et al., 2018; Ho and Ermon, 2016), adapting them to the large-scale language modelling setting. While alternative IRL methods often rely on nested optimisation loops between policy and reward, making them computationally prohibitive for LLMs, adversarial training provides a more tractable approach with close parallels to RLHF (Sun and van der Schaar, 2025). Our method jointly learns a reward model for reasoning and optimises the LLM policy against it, moving beyond standard supervised fine-tuning. Figure 1 summarises the approach: a discriminator LLM is trained as an implicit reward model via adversarial learning, and the reasoning policy is updated using the induced dense rewards.

4.1 Adversarial Learning of the Reasoning Reward Model

Let an output (reasoning trace) be $\tau = (y_{1:T})$ with tokens $y_t \in \mathcal{V}$. We denote by p_E the distribution over expert outputs and by p_θ the distribution over outputs induced by the current LLM policy π_θ. Inspired by GAIL (Ho and Ermon, 2016) and AIRL (Fu et al., 2018), we train a discriminator LLM D_ϕ (parameters ϕ) to distinguish expert from policy-generated outputs: $D_\phi(\tau) \in [0, 1]$ is the probability that τ came from p_E rather than p_θ. The discriminator is trained with the standard binary cross-entropy objective

$$\max_\phi \mathcal{L}_D(\phi) = \mathbb{E}_{\tau\sim p_E}\big[\log D_\phi(\tau)\big] + \mathbb{E}_{\tau\sim p_\theta}\big[\log\big(1 - D_\phi(\tau)\big)\big]. \tag{2}$$

For fixed p_θ, the optimal discriminator is (Goodfellow et al., 2014)

$$D_\phi^*(\tau) = \frac{p_E(\tau \mid x)}{p_E(\tau \mid x) + p_\theta(\tau \mid x)}, \tag{3}$$

which realises a density-ratio estimator between expert and policy distributions. Subsequently, we use the logit of the discriminator as an implicit reward to train the LLM reasoning policy τ_θ. In particular, at token position t with state $s_t = (x, y_{<t})$ and action y_t,

$$r_\phi(s_t, y_t) = r_\phi(y_t \mid x, y_{<t}) = \log D_\phi(y_t \mid x, y_{<t}) - \log\big(1 - D_\phi(y_t \mid x, y_{<t})\big), \tag{4}$$

yielding dense, token-level process feedback without explicit human reward annotation. For simplicity of notation, we will omit the condition in the reward and discriminator, and refer to it as $r_\phi(y_t)$ and $D_\phi(y_t)$, respectively.

4.2 Policy Learning with Dense Reasoning Rewards

Let $x \sim \mathcal{Q}$ denote a prompt drawn from the prompt distribution. For each x, we form a per-prompt group consisting of one expert demonstration $\tau^E \sim p_E(\cdot \mid x)$ (if available) and G policy candidates $\{\tau^{(g)}\}_{g=1}^G \sim p_{\theta_{\text{old}}}(\cdot \mid x)$, where $\tau^{(g)} = (y_{1:T_g}^{(g)})$. Applying (4) gives token-level rewards $r_\phi(y_t^{(g)}) \in \mathbb{R}$ for each sequence in the group.

To reduce variance and remove scale dependence, we normalise each reward within the group for prompt x. For any sequence τ in the group, define the baseline as the average reward of the last valid token in the sequence, as it encapsulates the information of the previous prompt and response tokens. Subsequently, we divide by the standard deviation of the rewards of the last valid token.

Let $\mathcal{S} = \{\tau^E\} \cup \{\tau^{(g)}\}_{g=1}^G$. Compute the standartisation as proposed for Group Relative Policy Optimisation (GRPO) by Zhao et al. (2024):

$$\bar{r} = \frac{1}{|\mathcal{S}|} \sum_{\tau \in \mathcal{S}_x} r_\phi(y_{T_\tau}), \qquad \sigma^2 = \frac{1}{|\mathcal{S}| - 1} \sum_{\tau \in \mathcal{S}} \big(r_\phi(y_{T_\tau}) - \bar{r}\big)^2$$

Standardised individual token rewards are $\tilde{r}_\phi(y_t) = \big(r_\phi(y_t) - \bar{r}\big)/\sigma$. Following the method proposed by Cui et al. (2025) for dense rewards, we define discounted advantages for each position t in a policy output $\tau^{(g)}$ as

$$A_t^{(g)} = \sum_{s=t}^{T_g} \gamma^{\,s-t}\, \tilde{r}_\phi(y_s^{(g)}), \qquad \gamma \in [0, 1]. \tag{5}$$

For completeness, the same construction yields A_t^E on the expert trace, and the policy updates uses $\{A_t^{(g)}\}_{g=1}^G$ and A_t^E, which can be seen as a weak form of supervised-finetuning, as the expert demonstration is anyways available. Once all the advantages A_t for every token are calculated, we update the policy with the Proximal Policy Optimisation clip surrogate loss (Schulman et al., 2017):

$$\min_\theta \mathcal{L}_{\text{clip}}(\theta) = \mathbb{E}_t\Big[\min\Big(\frac{\pi_\theta(y_t|x, y_{<t})}{\pi_{\theta_{\text{old}}}(y_t|x, y_{<t})} A_t, \text{clip}\Big(\frac{\pi_\theta(y_t|x, y_{<t})}{\pi_{\theta_{\text{old}}}(y_t|x, y_{<t})}, 1-\epsilon, 1+\epsilon\Big) A_t\Big)\Big] \tag{6}$$

An overview of the training can be found in Algorithm 1.

Algorithm 1 Adversarial inverse reinforcement learning for eliciting expert reasoning in LLMs

Require: Expert reasoning traces $\mathcal{D}_E = \{\tau_i^E\}_{i=1}^N$; number of iterations I

1: Initialise reasoning policy π_o and discriminator D_ϕ
2: **for** $i \leftarrow 1$ to I **do**
3: Generate G reasoning traces $\mathcal{D}_P \leftarrow \{\tau^{(g)}\}_{g=1}^G$ by sampling π_θ on prompts $x \sim \mathcal{Q}$
4: (Optionally) Add perturbed examples to $\mathcal{D}_P$
5: Update D_ϕ: maximise $\mathbb{E}_{\tau\sim\mathcal{D}_E}[\log D_\phi(\tau)] + \mathbb{E}_{\tau\sim\mathcal{D}_P}[\log\big(1 - D_\phi(\tau)\big)]$
6: Compute reward for each token in $\mathcal{S}$: $r_\phi(y_t^{(g)}) \leftarrow \log\big(D_\phi(y_t^{(g)})\big) - \log\big(1 - D_\phi(y_t^{(g)})\big)$
7: Normalise each reward $\tilde{r}_\phi(y_t^{(g)})$ and compute advantage score $A_t^{(g)}$
8: Optimise π_θ by applying one step of GRPO on $\mathcal{D}_\phi$ using rewards r_ϕ
9: **end for**

5 EXPERIMENTS

We evaluate on GSM8K (Cobbe et al., 2021), which includes human-annotated intermediate reasoning steps. Our base policies are open-weight, instruction-tuned variants not trained for reasoning: Qwen2.5 (policies: 3B, 7B; discriminators: 0.5B, 1.5B; Bai et al. (2023)) and Llama3 (policies: 3B, 8B; discriminator: 1B; Touvron et al. (2023)). Across different policy–discriminator pairings, we learn a dense, token-level reasoning reward from expert demonstrations and jointly optimise the policy with this reward. Evaluation follows the four desiderata from §1: (D1) reward as a training signal; (D2) inference-time assistance via critic-guided reranking under fixed sampling budgets; (D3) favouring likely-correct traces over stylistic conformity; and (D4) interpretable token-level diagnostics that localise errors. Implementation and optimisation details appear in Appendix A.

5.1 USING THE LEARNED REWARD AS A TRAINING SIGNAL

We first test whether the learned dense reasoning reward provides a useful signal for optimising a policy's step wise behaviour. We jointly train a policy and dense reasoning reward model on GSM8K and monitor (i) the mean reward assigned to full traces on evaluation data and (ii) the fraction of traces that end in a correct answer ("correctness accuracy") for both training and evaluation splits. Figure 2 shows the training dynamics for Llama3.1-8B with a Llama3.2-1B discriminator. The evaluation reward fluctuates from negative values toward zero and above, reflecting the adversarial interaction between the policy and the discriminator. The correctness accuracy increases, especially when the reward rises, and ends higher than before training.

We observe the same qualitative pattern across other policy and discriminator pairings, namely Qwen2.5 3B and 7B and Llama3 3B configurations, reported in Appendix B.1 Figures 7, 8, and 9. The evaluation reward tracks learning progress and is positively associated with correctness. This indicates that the discriminator's token-level supervision is not only fitting training data but also generalises as a process signal.

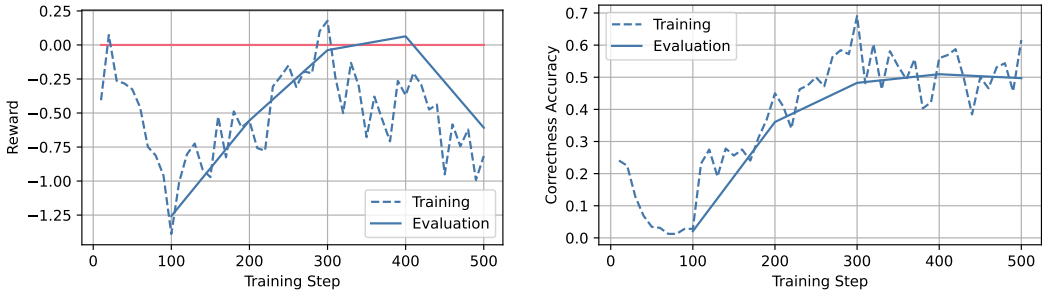

(a) Learned Rewards

(b) Correctness Accuracy

Figure 2: **Training behaviour of the reward and correctness** for Llama3.1-8B as the policy with Llama3.2-1B as the discriminator. Left (2a): aggregate learned reward over training steps (train/eval). Right (2b): correctness accuracy (train/eval).

For completeness, we benchmark predictive performance against two strong references in Appendix D.1: supervised fine-tuning on reasoning traces and GRPO (DeepSeek-AI et al., 2025), which uses verifiable outcome rewards and therefore serves as an empirical upper bound. Appendix Table 2 shows that our expert reasoning approach is frequently competitive with, and sometimes exceeds, supervised fine tuning across $k \in \{1, 3, 5, 10\}$, while GRPO traces the strongest curve. Closing the remaining gap to supervised fine tuning and GRPO in raw pass@1, without sacrificing the dual use of the learned reasoning reward model for training and inference, is promising future work.

Takeaway: The learned dense reward functions are a faithful training signal. Increases in the reward align with improvements in evaluation correctness. Although raw pass@1 can trail strong supervised fine tuning baselines and GRPO, the reasoning reward model's dual role enables capability gains that the following sections develop.

5.2 Inference Time Assistance via Reward-guided Reranking

We next test whether the learned reward can be used at inference to select better candidates from a small sample budget (Sun and van der Schaar, 2025). For each prompt we draw N candidate traces from the policy, score each trace by the mean discounted token level reward, and pick the top k traces by this score. We report pass@$k \mid N$, defined as the fraction of prompts for which at least one of the selected k traces is correct when N samples were available in total. Random ranking provides a natural baseline that does not use the reward. Unless stated otherwise we use $N = 16$.

Figure 3 shows results for Llama3.1-B with a Llama3.2-1B discriminator. The left panel displays the distribution of mean discounted rewards for answer tokens, split by whether the final answer is correct or not. The distributions are clearly separated with a large t statistic, and the right panel shows that reward guided reranking improves pass@$k \mid N$ over random ranking across the range of k. These results indicate that the reward model is calibrated to correctness and that its scores are useful for selection at inference.

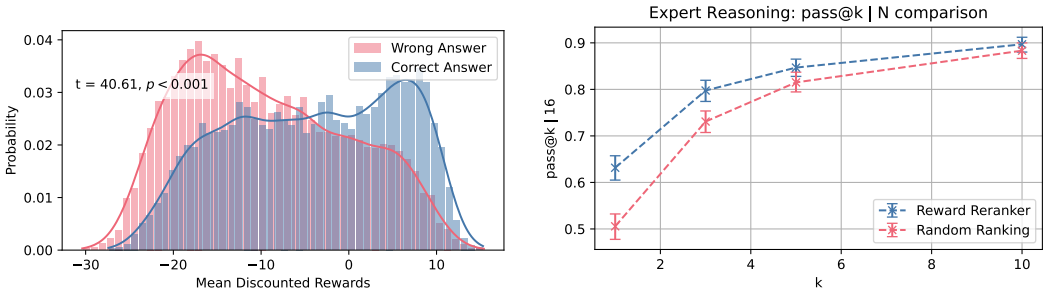

(a) Distribution of mean discounted rewards

(b) Comparison of pass@$k \mid N$

Figure 3: **Benefit of the reasoning reward at inference** for Llama3.1-8B with a Llama3.2-1B critic. Left(3a): reward distributions for correct versus incorrect answers. Right (3b): pass@$k \mid 16$ using reward-guided reranking versus random ranking.

Appendix B.2 reports the same analysis for Qwen2.5-3B and 7B and Llama3.2-3B in Figures 10, 11, and 12. For Llama3.2-3B, we again observe a clear separation of the reward distributions and consistent gains in pass@$k \mid 16$. For the Qwen models, reward-guided reranking does not yield statistically significant improvements. Two factors likely explain this outcome. First, the class conditional reward distributions overlap more for Qwen, which weakens the ranking signal. Second, the Qwen2.5 policies are already strong predictors (Table 2 shows Qwen2.5-7B exceeding SFT at pass@1), leaving limited headroom for selection to change the top k. Consequently, the marginal value of reranking is potentially reduced, even when the distributional separation is statistically non-zero.

> **Takeaway:** The learned reward is effective for inference time selection under a fixed budget, with clear pass@$k \mid N$ gains for Llama3-based policies. For Qwen2.5, despite a statistically significant separation of reward distributions, reranking does not produce significant gains, likely due to the strong base accuracy and weaker separation.

5.3 Reward prefers likely correct traces over stylistic conformity

In this experiment, we investigate whether the learned reward is based on correctness rather than superficial formatting. For each response, we compute the mean (discounted) reward over answer tokens and compare it to verifiable signals used in GRPO: a binary correctness indicator and a formatting or structure signal. We report Pearson correlations.

Figure 4 shows the correlation matrix for the Llama3.1-8B policy with Llama3.2-1B discriminator. The learned (discounted) rewards exhibit their strongest association with correctness ($\rho = 0.27$ for rewards, and $\rho = 0.30$ for discounted rewards, $\gamma = 0.9$). At the same time, correlations with formatting-based signals (XML Count, Strict Format, Soft Format, and integer response) are appreciably smaller. This pattern indicates that the reasoning reward model scores are calibrated to solution validity rather than to the presence of a particular structure, which is consistent with the separation observed in the reward distributions and with the improvements from reranking in subsection 5.2. Additional correlation matrices for other backbones are reported in Appendix B.3 in Figure 13.

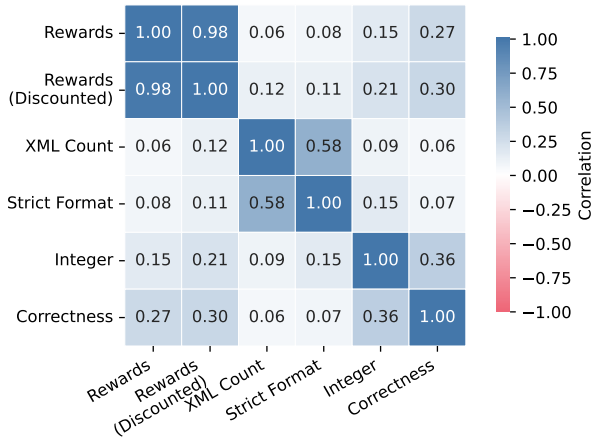

Figure 4: **Correlation of the learned reward** for Llama3.1-8B with Llama3.2-1B. Shows correlations between the (discounted) learned reward on answer tokens and verifiable signals: correctness and formatting structure.

To improve robustness, we introduce perturbed samples during training for both expert and policy traces. The perturbations flip operator signs, corrupt numbers, and swap the final answer with a previous intermediate number. The perturbations expose near-miss errors that share surface form with correct traces but are semantically incorrect. In Appendix D.3, we report our experiment comparing training with and without perturbations in Figure 25. With perturbations, the reward distributions for correct and incorrect answers separate more clearly, the pass@$k \mid N$ curves improve at low k, and the correlations with formatting signals decreases.

> **Takeaway:** The learned reward correlates most strongly with correctness and only weakly with formatting, indicating a preference for likely correct traces rather than stylistic conformity. Training with targeted perturbations further sharpens this preference and improves selection behaviour.

5.4 Interpretable dense rewards and localisation of errors

We evaluate whether the learned dense reward provides actionable interpretability by revealing where a reasoning trace succeeds or fails. We visualise token-level normalised rewards along the trace and focus on the answer region with discount factor $\gamma = 0.9$. Here, we display one correct and one incorrect example for Llama3.1-8B with a Llama3.2-1B discriminator (Figures 5 and 6); the appendix provides two additional correct and two additional incorrect examples per backbone for both Llama3 and Qwen2.5 combination (Appendix B.4, Figures 14, 15, and 16).

In correct solutions the reward forms contiguous positive bands that align with decisive computations and algebraic simplifications, with neutral or slightly positive rewards on connective tokens. In incorrect solutions we observe early negative bands at the point of deviation, followed by persistently negative or oscillating rewards. The penalties propagate forward due to discounting, which makes the final answer region strongly negative even when surface level formatting remains plausible. These patterns are consistent across backbones and mirror the distributional separation and reranking gains reported in subsections 5.1 and 5.2.

> **Takeaway:** The learned dense reward yields interpretable token-level attributions that pinpoint failure and reveal error propagation, enabling auditing and simple triggers for early rejection or self-revision. A natural extension and interesting option for future work is reward-guided next-token generation to self-correct when a trace begins to drift.

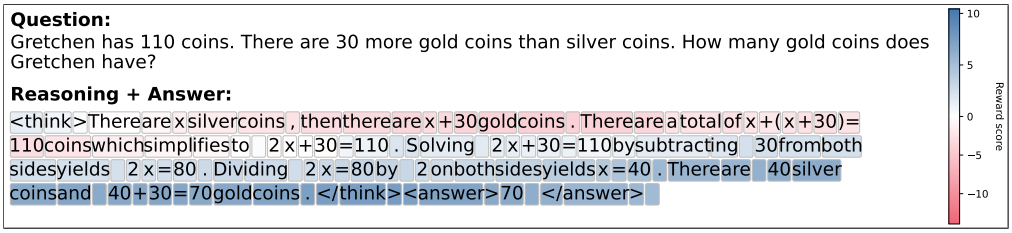

Figure 5: **Correct answering.** Dense reward on a correct solution shows contiguous positive bands on decisive computations. Rewards are standardised and discounted with $\gamma = 0.9$.

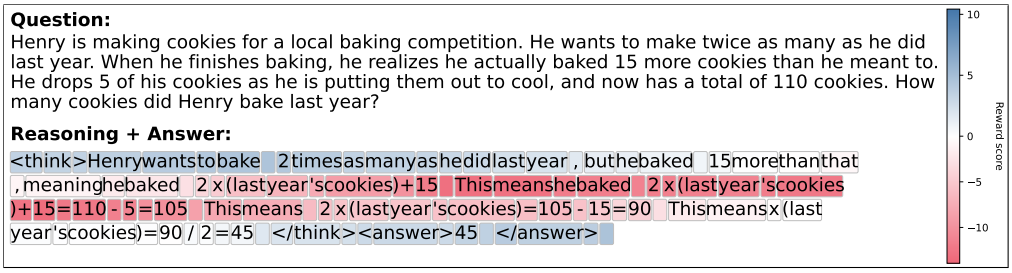

Figure 6: **Incorrect answering.** Dense reward on an incorrect solution highlights the first erroneous step with a sharp negative band, followed by propagated penalties into later tokens and the final answer due to discounting. Rewards are standardised and discounted with $\gamma = 0.9$.

6 Limitations

Our approach has several limitations. Joint optimisation of the policy and the learned reward can lag SFT on some backbones in pass@1. The discriminator may inherit bias or noise from expert traces, and adversarial training yields non-stationary signals. Learned rewards can overfit to superficial cues, and calibration differs across model families, with weaker separation in Qwen2.5 than in Llama3. Performance depends on choices such as discounting, token aggregation, and normalisation. Compute and latency rise due to alternating updates and inference-time scoring. Finally, evaluation is limited to GSM8K-style arithmetic reasoning and does not cover long context, multimodality, or high-stakes settings.

7 Future Work

A learned dense reward can serve as both a training signal and an inference-time assistant, providing token-level diagnostics. Several directions follow. First, close the remaining pass@1 gap to strong SFT by improving optimisation at the discriminator–policy interface; to this end we also explored a Wasserstein GAN (Arjovsky et al., 2017) variant (Appendix D.4). Second, improve reward calibration across backbones, especially Qwen2.5, by refining perturbations, using hard negatives, and adopting contrastive objectives. Third, integrate the critic at generation time through reward-guided decoding, early rejection, and self-revision. Fourth, extend beyond GSM8K to broader domains and to settings with limited or noisy demonstrations, including online learning and active data collection.

8 Conclusion

We introduced an inverse reinforcement learning approach that learns a dense reasoning reward from expert demonstrations. The learned critic serves two roles. It teaches a policy to reason from token-level feedback and improves predictive performance at inference by reranking under a fixed sampling budget. The reward aligns with correctness rather than surface form and offers interpretable localisation of errors. While raw accuracy may trail strong supervised fine-tuning and outcome-reward RL, the capability gains are clear. We view this work as a step toward reusable process-level critics that support training, inference, and diagnosis in a single framework.

REFERENCES

DeepSeek-AI, Daya Guo, Dejian Yang, Haowei Zhang, Junxiao Song, Ruoyu Zhang, Runxin Xu, Qihao Zhu, Shirong Ma, Peiyi Wang, Xiao Bi, Xiaokang Zhang, Xingkai Yu, Yu Wu, Z. F. Wu, Zhibin Gou, Zhihong Shao, Zhuoshu Li, Ziyi Gao, Aixin Liu, Bing Xue, Bingxuan Wang, Bochao Wu, Bei Feng, Chengda Lu, Chenggang Zhao, Chengqi Deng, Chenyu Zhang, Chong Ruan, Damai Dai, Deli Chen, Dongjie Ji, Erhang Li, Fangyun Lin, Fucong Dai, Fuli Luo, Guangbo Hao, Guanting Chen, Guowei Li, H. Zhang, Han Bao, Hanwei Xu, Haocheng Wang, Honghui Ding, Huajian Xin, Huazuo Gao, Hui Qu, Hui Li, Jianzhong Guo, Jiashi Li, Jiawei Wang, Jingchang Chen, Jingyang Yuan, Junjie Qiu, Junlong Li, J. L. Cai, Jiaqi Ni, Jian Liang, Jin Chen, Kai Dong, Kai Hu, Kaige Gao, Kang Guan, Kexin Huang, Kuai Yu, Lean Wang, Lecong Zhang, Liang Zhao, Litong Wang, Liyue Zhang, Lei Xu, Leyi Xia, Mingchuan Zhang, Minghua Zhang, Minghui Tang, Meng Li, Miaojun Wang, Mingming Li, Ning Tian, Panpan Huang, Peng Zhang, Qiancheng Wang, Qinyu Chen, Qiushi Du, Ruiqi Ge, Ruisong Zhang, Ruizhe Pan, Runji Wang, R. J. Chen, R. L. Jin, Ruyi Chen, Shanghao Lu, Shangyan Zhou, Shanhuang Chen, Shengfeng Ye, Shiyu Wang, Shuiping Yu, Shunfeng Zhou, Shuting Pan, S. S. Li, Shuang Zhou, Shaoqing Wu, Shengfeng Ye, Tao Yun, Tian Pei, Tianyu Sun, T. Wang, Wangding Zeng, Wanjia Zhao, Wen Liu, Wenfeng Liang, Wenjun Gao, Wenqin Yu, Wentao Zhang, W. L. Xiao, Wei An, Xiaodong Liu, Xiaohan Wang, Xiaokang Chen, Xiaotao Nie, Xin Cheng, Xin Liu, Xin Xie, Xingchao Liu, Xinyu Yang, Xinyuan Li, Xuecheng Su, Xuheng Lin, X. Q. Li, Xiangyue Jin, Xiaojin Shen, Xiaosha Chen, Xiaowen Sun, Xiaoxiang Wang, Xinnan Song, Xinyi Zhou, Xianzu Wang, Xinxia Shan, Y. K. Li, Y. Q. Wang, Y. X. Wei, Yang Zhang, Yanhong Xu, Yao Li, Yao Zhao, Yaofeng Sun, Yaohui Wang, Yi Yu, Yichao Zhang, Yifan Shi, Yiliang Xiong, Ying He, Yishi Piao, Yisong Wang, Yixuan Tan, Yiyang Ma, Yiyuan Liu, Yongqiang Guo, Yuan Ou, Yuduan Wang, Yue Gong, Yuheng Zou, Yujia He, Yunfan Xiong, Yuxiang Luo, Yuxiang You, Yuxuan Liu, Yuyang Zhou, Y. X. Zhu, Yanhong Xu, Yanping Huang, Yaohui Li, Yi Zheng, Yuchen Zhu, Yunxian Ma, Ying Tang, Yukun Zha, Yuting Yan, Z. Z. Ren, Zehui Ren, Zhangli Sha, Zhe Fu, Zhean Xu, Zhenda Xie, Zhengyan Zhang, Zhewen Hao, Zhicheng Ma, Zhigang Yan, Zhiyu Wu, Zihui Gu, Zijia Zhu, Zijun Liu, Zilin Li, Ziwei Xie, Ziyang Song, Zizheng Pan, Zhen Huang, Zhipeng Xu, Zhongyu Zhang, and Zhen Zhang. DeepSeek-R1: Incentivizing Reasoning Capability in LLMs via Reinforcement Learning, January 2025. URL http://arxiv.org/abs/2501.12948. arXiv:2501.12948 [cs].

Amrith Setlur, Nived Rajaraman, Sergey Levine, and Aviral Kumar. Scaling Test-Time Compute Without Verification or RL is Suboptimal, February 2025. URL http://arxiv.org/abs/2502.12118. arXiv:2502.12118 [cs].

Hao Sun and Mihaela van der Schaar. Inverse-RLignment: Large Language Model Alignment from Demonstrations through Inverse Reinforcement Learning, January 2025. URL http://arxiv.org/abs/2405.15624. arXiv:2405.15624 [cs].

Jonathan Uesato, Nate Kushman, Ramana Kumar, Francis Song, Noah Siegel, Lisa Wang, Antonia Creswell, Geoffrey Irving, and Irina Higgins. Solving math word problems with process- and outcome-based feedback, November 2022. URL http://arxiv.org/abs/2211.14275. arXiv:2211.14275 [cs].

Hunter Lightman, Vineet Kosaraju, Yura Burda, Harri Edwards, Bowen Baker, Teddy Lee, Jan Leike, John Schulman, Ilya Sutskever, and Karl Cobbe. Let's Verify Step by Step, May 2023. URL http://arxiv.org/abs/2305.20050. arXiv:2305.20050 [cs].

Eric Zelikman, Yuhuai Wu, Jesse Mu, and Noah D. Goodman. STaR: Bootstrapping Reasoning With Reasoning, May 2022. URL http://arxiv.org/abs/2203.14465. arXiv:2203.14465 [cs].

Zheng Yuan, Hongyi Yuan, Chengpeng Li, Guanting Dong, Keming Lu, Chuanqi Tan, Chang Zhou, and Jingren Zhou. Scaling Relationship on Learning Mathematical Reasoning with Large Language Models, September 2023. URL http://arxiv.org/abs/2308.01825. arXiv:2308.01825 [cs].

Avi Singh, John D. Co-Reyes, Rishabh Agarwal, Ankesh Anand, Piyush Patil, Xavier Garcia, Peter J. Liu, James Harrison, Jaehoon Lee, Kelvin Xu, Aaron T. Parisi, Abhishek Kumar, Alexander A. Alemi, Alex Rizkowsky, Azade Nova, Ben Adlam, Bernd Bohnet, Gamaleldin Fathy Elsayed,

Hanie Sedghi, Igor Mordatch, Isabelle Simpson, Izzeddin Gur, Jasper Snoek, Jeffrey Pennington, Jiri Hron, Kathleen Kenealy, Kevin Swersky, Kshiteej Mahajan, Laura A. Culp, Lechao Xiao, Maxwell Bileschi, Noah Constant, Roman Novak, Rosanne Liu, Tris Warkentin, Yamini Bansal, Ethan Dyer, Behnam Neyshabur, Jascha Sohl-Dickstein, and Noah Fiedel. Beyond Human Data: Scaling Self-Training for Problem-Solving with Language Models. *Transactions on Machine Learning Research*, January 2024. ISSN 2835-8856. URL https://openreview.net/forum?id=lNAyUngGFK.

Arian Hosseini, Xingdi Yuan, Nikolay Malkin, Aaron Courville, Alessandro Sordoni, and Rishabh Agarwal. V-STaR: Training Verifiers for Self-Taught Reasoners. August 2024. URL https://openreview.net/forum?id=stmqBSW2dV#discussion.

David Silver, Julian Schrittwieser, Karen Simonyan, Ioannis Antonoglou, Aja Huang, Arthur Guez, Thomas Hubert, Lucas baker, Matthew Lai, Adrian Bolton, Yutian Chen, Timothy P. Lillicrap, Fan Hui, L. Sifre, George van den Driessche, Thore Graepel, and Demis Hassabis. Mastering the game of go without human knowledge. *Nature*, 550:354–359, 2017. URL https://api.semanticscholar.org/CorpusID:205261034.

Ganqu Cui, Lifan Yuan, Zefan Wang, Hanbin Wang, Wendi Li, Bingxiang He, Yuchen Fan, Tianyu Yu, Qixin Xu, Weize Chen, Jiarui Yuan, Huayu Chen, Kaiyan Zhang, Xingtai Lv, Shuo Wang, Yuan Yao, Xu Han, Hao Peng, Yu Cheng, Zhiyuan Liu, Maosong Sun, Bowen Zhou, and Ning Ding. Process Reinforcement through Implicit Rewards, February 2025. URL http://arxiv.org/abs/2502.01456. arXiv:2502.01456 [cs].

Rafael Rafailov, Archit Sharma, Eric Mitchell, Stefano Ermon, Christopher D. Manning, and Chelsea Finn. Direct Preference Optimization: Your Language Model is Secretly a Reward Model, July 2024. URL http://arxiv.org/abs/2305.18290. arXiv:2305.18290.

Brian D Ziebart, Andrew Maas, J Andrew Bagnell, and Anind K Dey. Maximum Entropy Inverse Reinforcement Learning. 2004.

Pieter Abbeel and Andrew Y. Ng. Apprenticeship learning via inverse reinforcement learning. In *Twenty-first international conference on Machine learning - ICML '04*, page 1, Banff, Alberta, Canada, 2004. ACM Press. doi: 10.1145/1015330.1015430. URL http://portal.acm.org/citation.cfm?doid=1015330.1015430.

Joey Hejna and Dorsa Sadigh. Inverse Preference Learning: Preference-based RL without a Reward Function. 2023.

Justin Fu, Anoop Korattikara, Sergey Levine, and Sergio Guadarrama. FROM LANGUAGE TO GOALS: INVERSE REINFORCE- MENT LEARNING FOR VISION-BASED INSTRUCTION FOLLOWING. 2019.

Jonathan Ho and Stefano Ermon. Generative Adversarial Imitation Learning, June 2016. URL http://arxiv.org/abs/1606.03476. arXiv:1606.03476 [cs].

Paul Christiano, Jan Leike, Tom B. Brown, Miljan Martic, Shane Legg, and Dario Amodei. Deep reinforcement learning from human preferences, February 2023. URL http://arxiv.org/abs/1706.03741. arXiv:1706.03741.

Hao Sun and Mihaela van der Schaar. Inverse-RLignment: Inverse Reinforcement Learning from Demonstrations for LLM Alignment, May 2024. URL http://arxiv.org/abs/2405.15624. arXiv:2405.15624 [cs].

Han Xia, Songyang Gao, Qiming Ge, Zhiheng Xi, Qi Zhang, and Xuanjing Huang. Inverse-Q*: Token Level Reinforcement Learning for Aligning Large Language Models Without Preference Data, August 2024. URL http://arxiv.org/abs/2408.14874. arXiv:2408.14874 [cs].

Hao Sun and Mihaela van der Schaar. Inverse Reinforcement Learning Meets Large Language Model Post-Training: Basics, Advances, and Opportunities, July 2025. URL http://arxiv.org/abs/2507.13158. arXiv:2507.13158 [cs].

Jared Joselowitz, Arjun Jagota, Satyapriya Krishna, and Sonali Parbhoo. Insights from the Inverse: Reconstructing LLM Training Goals Through Inverse RL, October 2024. URL http://arxiv.org/abs/2410.12491. arXiv:2410.12491 [cs].

Justin Fu, Katie Luo, and Sergey Levine. Learning Robust Rewards with Adversarial Inverse Reinforcement Learning, August 2018. URL http://arxiv.org/abs/1710.11248. arXiv:1710.11248 [cs].

Jiahao Lin and Zongzhang Zhang. ACGAIL: Imitation Learning About Multiple Intentions with Auxiliary Classifier GANs. In Xin Geng and Byeong-Ho Kang, editors, *PRICAI 2018: Trends in Artificial Intelligence*, pages 321–334, Cham, 2018. Springer International Publishing. ISBN 978-3-319-97304-3. doi: 10.1007/978-3-319-97304-3_25.

Yunzhu Li, Jiaming Song, and Stefano Ermon. InfoGAIL: Interpretable Imitation Learning from Visual Demonstrations, November 2017. URL http://arxiv.org/abs/1703.08840. arXiv:1703.08840 [cs].

Geoffrey Hinton, Oriol Vinyals, and Jeff Dean. Distilling the Knowledge in a Neural Network, March 2015. URL http://arxiv.org/abs/1503.02531. arXiv:1503.02531 [stat].

Minki Kang, Seanie Lee, Jinheon Baek, Kenji Kawaguchi, and Sung Ju Hwang. Knowledge-Augmented Reasoning Distillation for Small Language Models in Knowledge-Intensive Tasks. In A. Oh, T. Naumann, A. Globerson, K. Saenko, M. Hardt, and S. Levine, editors, *Advances in Neural Information Processing Systems*, volume 36, pages 48573–48602. Curran Associates, Inc., 2023. URL https://proceedings.neurips.cc/paper_files/paper/2023/file/97faedc90260eae5c400f92d5831c3d7-Paper-Conference.pdf.

Kalle Kujanpää, Pekka Marttinen, Harri Valpola, and Alexander Ilin. Efficient Knowledge Injection in LLMs via Self-Distillation, August 2025. URL http://arxiv.org/abs/2412.14964. arXiv:2412.14964 [cs].

Hongling Xu, Qi Zhu, Heyuan Deng, Jinpeng Li, Lu Hou, Yasheng Wang, Lifeng Shang, Ruifeng Xu, and Fei Mi. KDRL: Post-Training Reasoning LLMs via Unified Knowledge Distillation and Reinforcement Learning, June 2025. URL http://arxiv.org/abs/2506.02208. arXiv:2506.02208 [cs].

Ian J. Goodfellow, Jean Pouget-Abadie, Mehdi Mirza, Bing Xu, David Warde-Farley, Sherjil Ozair, Aaron Courville, and Yoshua Bengio. Generative Adversarial Networks, June 2014. URL http://arxiv.org/abs/1406.2661. arXiv:1406.2661 [stat].

Siyan Zhao, John Dang, and Aditya Grover. Group Preference Optimization: Few-Shot Alignment of Large Language Models, October 2024. URL http://arxiv.org/abs/2310.11523. arXiv:2310.11523.

John Schulman, Filip Wolski, Prafulla Dhariwal, Alec Radford, and Oleg Klimov. Proximal Policy Optimization Algorithms, August 2017. URL http://arxiv.org/abs/1707.06347. arXiv:1707.06347 [cs].

Karl Cobbe, Vineet Kosaraju, Mohammad Bavarian, Mark Chen, Heewoo Jun, Lukasz Kaiser, Matthias Plappert, Jerry Tworek, Jacob Hilton, Reiichiro Nakano, Christopher Hesse, and John Schulman. Training Verifiers to Solve Math Word Problems, November 2021. URL http://arxiv.org/abs/2110.14168. arXiv:2110.14168 [cs].

Jinze Bai, Shuai Bai, Yunfei Chu, Zeyu Cui, Kai Dang, Xiaodong Deng, Yang Fan, Wenbin Ge, Yu Han, Fei Huang, Binyuan Hui, Luo Ji, Mei Li, Junyang Lin, Runji Lin, Dayiheng Liu, Gao Liu, Chengqiang Lu, Keming Lu, Jianxin Ma, Rui Men, Xingzhang Ren, Xuancheng Ren, Chuanqi Tan, Sinan Tan, Jianhong Tu, Peng Wang, Shijie Wang, Wei Wang, Shengguang Wu, Benfeng Xu, Jin Xu, An Yang, Hao Yang, Jian Yang, Shusheng Yang, Yang Yao, Bowen Yu, Hongyi Yuan, Zheng Yuan, Jianwei Zhang, Xingxuan Zhang, Yichang Zhang, Zhenru Zhang, Chang Zhou, Jingren Zhou, Xiaohuan Zhou, and Tianhang Zhu. Qwen Technical Report, September 2023. URL http://arxiv.org/abs/2309.16609. arXiv:2309.16609 [cs].

Hugo Touvron, Thibaut Lavril, Gautier Izacard, Xavier Martinet, Marie-Anne Lachaux, Timothée Lacroix, Baptiste Rozière, Naman Goyal, Eric Hambro, Faisal Azhar, Aurelien Rodriguez, Armand Joulin, Edouard Grave, and Guillaume Lample. LLaMA: Open and Efficient Foundation Language Models, February 2023. URL http://arxiv.org/abs/2302.13971. arXiv:2302.13971 [cs].

Martin Arjovsky, Soumith Chintala, and Léon Bottou. Wasserstein GAN, December 2017. URL http://arxiv.org/abs/1701.07875. arXiv:1701.07875 [stat].

Guido Van Rossum and Fred L Drake Jr. *Python reference manual*. Centrum voor Wiskunde en Informatica Amsterdam, 1995.

Adam Paszke, Sam Gross, Soumith Chintala, Gregory Chanan, Edward Yang, Zachary DeVito, Zeming Lin, Alban Desmaison, Luca Antiga, and Adam Lerer. Automatic differentiation in pytorch. 2017.

Thomas Wolf, Lysandre Debut, Victor Sanh, Julien Chaumond, Clement Delangue, Anthony Moi, Pierric Cistac, Tim Rault, Rémi Louf, Morgan Funtowicz, Joe Davison, Sam Shleifer, Patrick von Platen, Clara Ma, Yacine Jernite, Julien Plu, Canwen Xu, Teven Le Scao, Sylvain Gugger, Mariama Drame, Quentin Lhoest, and Alexander M. Rush. HuggingFace's Transformers: State-of-the-art Natural Language Processing, July 2020. URL http://arxiv.org/abs/1910.03771. arXiv:1910.03771 [cs].

Michael Han Daniel Han and Unsloth team. Unsloth, 2023. URL http://github.com/unslothai/unsloth.

Juncheng Wu, Wenlong Deng, Xingxuan Li, Sheng Liu, Taomian Mi, Yifan Peng, Ziyang Xu, Yi Liu, Hyunjin Cho, Chang-In Choi, Yihan Cao, Hui Ren, Xiang Li, Xiaoxiao Li, and Yuyin Zhou. Medreason: Eliciting factual medical reasoning steps in llms via knowledge graphs, 2025. URL https://arxiv.org/abs/2504.00993.

Di Jin, Eileen Pan, Nassim Oufattole, Wei-Hung Weng, Hanyi Fang, and Peter Szolovits. What disease does this patient have? a large-scale open domain question answering dataset from medical exams. *Applied Sciences*, 11(14):6421, 2021.

Ankit Pal, Logesh Kumar Umapathi, and Malaikannan Sankarasubbu. Medmcqa: A large-scale multi-subject multi-choice dataset for medical domain question answering. In Gerardo Flores, George H Chen, Tom Pollard, Joyce C Ho, and Tristan Naumann, editors, *Proceedings of the Conference on Health, Inference, and Learning*, volume 174 of *Proceedings of Machine Learning Research*, pages 248–260. PMLR, 07–08 Apr 2022. URL https://proceedings.mlr.press/v174/pal22a.html.

A Implementation Details

We evaluate the proposed expert reasoning approach on GSM8K, a benchmark of grade school mathematics problems that provides final answers and human-written demonstrations. Unless noted otherwise, we use open-weight instruction-tuned models as base policies and train a learned reward using adversarial inverse reinforcement learning. When the reward model is implemented as a sequence classifier, it yields a sparse signal at the sequence level. To obtain a dense signal, we instead implement the discriminator as a token classifier that shares the backbone with a language model and replaces the language modelling head with a single linear layer that outputs one logit per token. The code to all our experiments can be found at https://anonymous.4open.science/r/expert_reasoning-C1E8.

All experiments are implemented in Python (Van Rossum and Drake Jr, 1995) with PyTorch (Paszke et al., 2017) and Hugging Face Transformers (Wolf et al., 2020). We accelerate training and evaluation with Unsloth (Daniel Han and team, 2023). Unless stated otherwise we use a starting learning rate of 1×10^{-5} for both policy and discriminator (1×10^{-4} for the Llama models) with a cosine schedule and ten per cent warm up. We train for 500 optimisation steps with batch size 16 and generate $G = 16$ samples per prompt, accumulated over two gradient steps.

Data and preprocessing. We follow the standard GSM8K split. Prompts consist of the problem text with a short system instruction that requests step by step reasoning. Demonstrations are formatted as `<think> ... </think>` followed by `<answer> ... </answer>` format. Tokenisation uses the native tokeniser of each backbone. For evaluation, we decode with temperature $T = 1.0$ and $\texttt{top\_p} = 0.95$ unless stated otherwise.

Objectives and optimisation. The discriminator is trained with a binary cross entropy objective to distinguish expert traces from policy traces at the token level. Let $r_\phi(y_t \mid x, y_{<t})$ denote the reward at token t; the aggregate trace reward is the mean of discounted rewards over the answer segment with discount factor $\gamma = 0.9$. Policy updates follow a group wise normalised advantage objective with G samples per prompt. We apply gradient clipping, weight decay ($\beta_1 = 0.9$, $\beta_2 = 0.99$), and label smoothing (0.95) on the discriminator targets. We use a quantised ADAM optimiser.

Inference time scoring. At inference we draw $N = 16$ samples per prompt, compute the mean discounted reward over answer tokens for each sample, and rerank by this score. We report pass@k | N, the fraction of prompts for which at least one of the top k ranked samples is correct when N samples are available. Unless noted otherwise $N = 16$ and $k \in \{1, 3, 5, 10\}$.

Perturbations. To improve robustness and reduce reliance on surface form we introduce targeted perturbations during discriminator training for both expert and policy traces: (i) flip arithmetic operator signs, (ii) corrupt numeric literals by small random offsets, and (iii) swap the final answer with an earlier intermediate number. Perturbed traces are labelled as non expert.

Compute. Experiments are conducted on A100-class GPUs with mixed-precision training. We use gradient accumulation to match effective batch sizes across backbones. All models are in 4-bit mode, provided by UNSLOTH (Daniel Han and team, 2023) for training speed and memory efficiency.

A.1 Policy Model

Policies are initialised from instruction-tuned checkpoints and trained with the learned reward signal. The following policy backbones are used:

- `Llama3.1-8B-Instruct`
- `Llama3.2-3B-Instruct`
- `Qwen 2.5-3B-Instruct`
- `Qwen 2.5-7B-Instruct`

A.2 Discriminator Model

Unless specified otherwise the discriminator shares the architecture family with the policy but differs in size. The discriminator is always trained as a token classifier:

- `Llama3.2-1B-Instruct`
- `Qwen-2.5-0.5B-Instruct`
- `Qwen-2.5-1.5B-Instruct`
- `Qwen-2.5-Math-1.5B-Instruct` (*ablation*)

A.3 Policy–discriminator combinations

We evaluate the following pairings; results for the representative configuration appear in the main text, and the remainder in the appendix:

Policy	**Discriminator**
`Llama3.1-8B-Instruct`	`Llama3.2-1B-Instruct`
`Llama3.2-3B-Instruct`	`Llama3.2-3B-Instruct`
`Qwen-2.5-3B-Instruct`	`Qwen-2.5-0.5B-Instruct`
`Qwen-2.5-7B-Instruct`	`Qwe-2.5-1.5B-Instruct`
`Qwen-2.5-7B-Instruct`	`Qwen-2.5-0.5B-Instruct` *(ablation)*
`Qwen-2.5-7B-Instruct`	`Qwen-2.5-Math-1.5B-Instruct` *(ablation)*

For completeness, we also test a maths-specialised variant of the discriminator within the Qwen family; it does not improve calibration relative to the general-purpose discriminator in our setting and is therefore reported only in the Appendix D.2.

A.4 Statement about the Use of Large Language Models

We utilised large language models to assist with drafting and editing the manuscript, as well as to accelerate implementation by generating boilerplate code and providing debugging suggestions. LLMs were not involved in the conception of the methods, study design, or interpretation of results. All outputs were reviewed and verified by the authors, who take full responsibility for the content.

B Additional Results

B.1 Training Behaviour

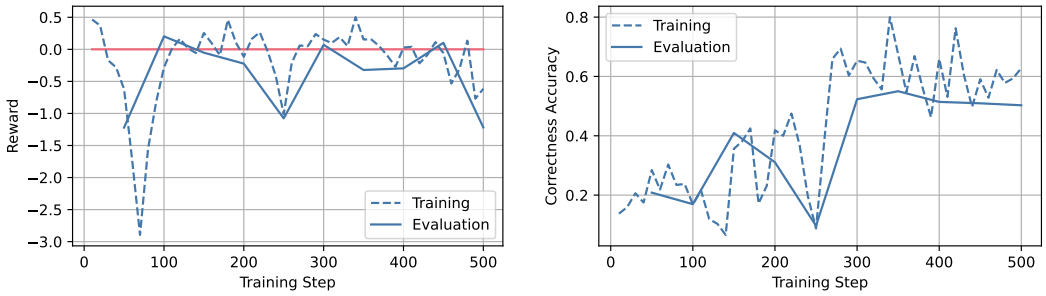

(a) Learned Rewards (b) Correctness Accuracy

Figure 7: **Training behaviour of the Reward and Correctness.** Subfigure 7a shows the training and evaluation reward during optimisation, and Subfigure 7b demonstrates the increasing correctness for the (`Qwen2.5-3B-Instruct - Qwen2.5-0.5B-Instruct`) combination.

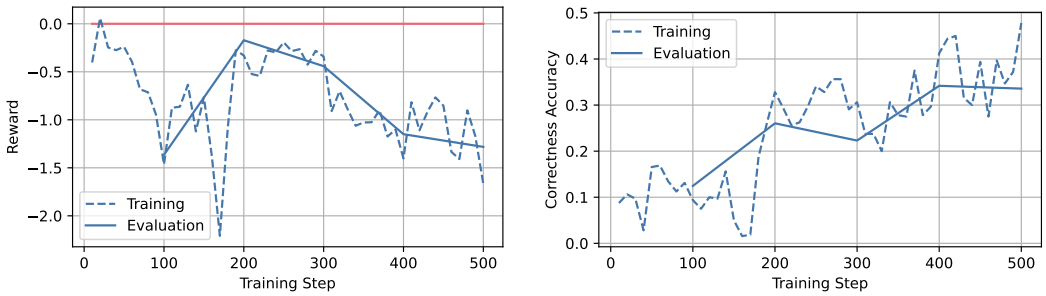

(a) Learned Rewards (b) Correctness Accuracy

Figure 8: **Training behaviour of the Reward and Correctness.** Subfigure 8a shows the training and evaluation reward during optimisation, and Subfigure 8b demonstrates the increasing correctness for the (`Llama3.1-3B-Instruct - Llama3.2-1B-Instruct`) combination.

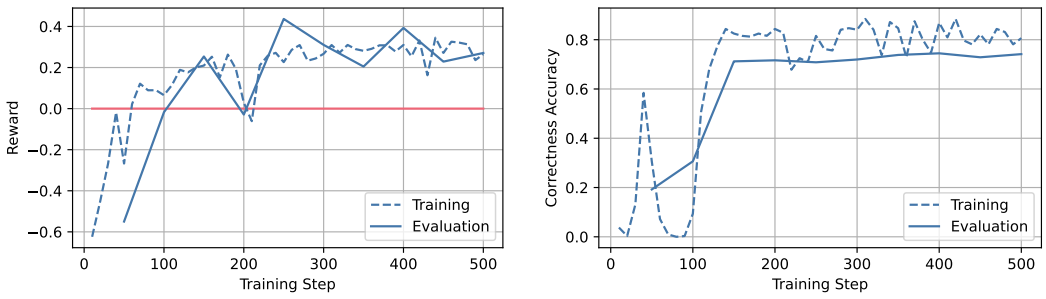

(a) Learned Rewards (b) Correctness Accuracy

Figure 9: **Training behaviour of the Reward and Correctness.** Subfigure 9a shows the training and evaluation reward during optimisation, and Subfigure 9b demonstrates the increasing correctness for the (`Qwen2.5-7B-Instruct - Qwen2.5-1.5B-Instruct`) combination.

B.2 Distribution of Rewards and Reranking Performance

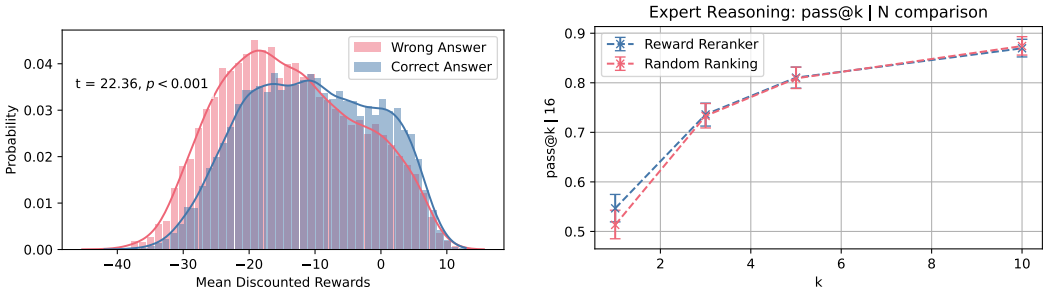

(a) Distribution of mean discounted (b) Pass@k|N

Figure 10: **Benefit of Reasoning Reward Model.** This is for the (`Qwen2.5-3B-Instruct` - `Qwen2.5-0.5B-Instruct`) combination.

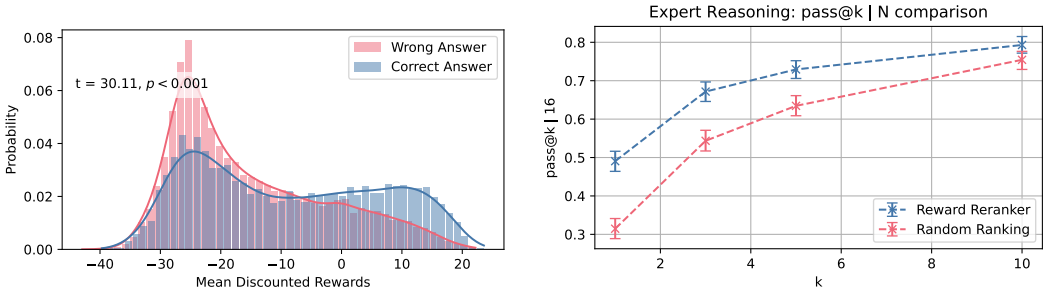

(a) Distribution of mean discounted rewards (b) Pass@k|N

Figure 11: **Benefit of Reasoning Reward Model.** This is for the (`Llama3.2-3B-Instruct` - `Llama3.2-1B-Instruct`) combination.

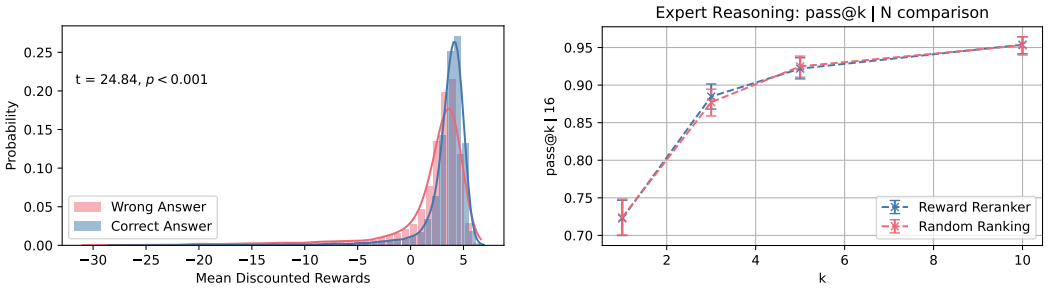

(a) Distribution of mean discounted rewards (b) Pass@k|N

Figure 12: **Benefit of Reasoning Reward Model.** This is for the (`Qwen2.5-7B-Instruct` - `Qwen2.5-1.5B-Instruct`) combination.

B.3 Correlation of Reward Model with Correctness and Formatting

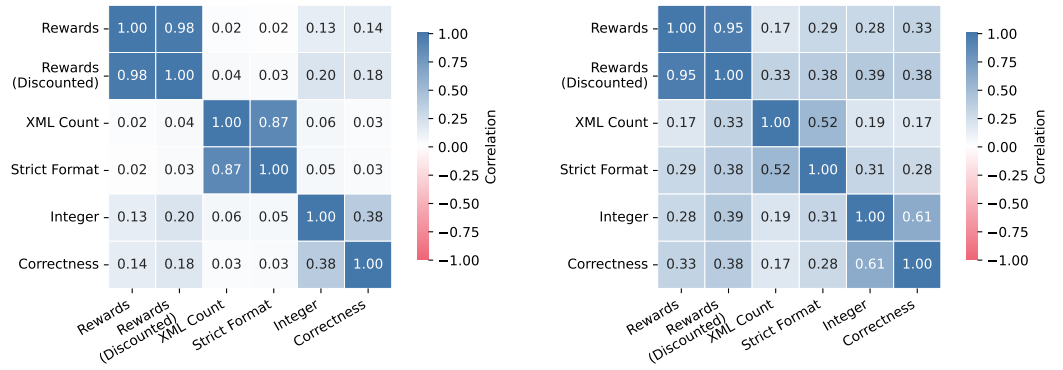

(a) (`Qwen2.5-3B-Instruct` - `Qwen2.5-0.5B-Instruct`)

(b) (`Llama3.2-3B-Instruct` - `Llama3.2-1B-Instruct`)

(c) (`Qwen2.5-7B-Instruct` - `Qwen2.5-1.5B-Instruct`)

(d) (`Llama3.1-8B-Instruct` - `Llama3.2-1B-Instruct`)

Figure 13: **Correlation Matrix of Verifiable Rewards with Learned Reward.** Correlation between the mean rewards of the answer tokens with the various verifiable rewards, used in GRPO training. We are especially interested in the correlation between correctness and the rewards.

B.4 REASONING TRACES

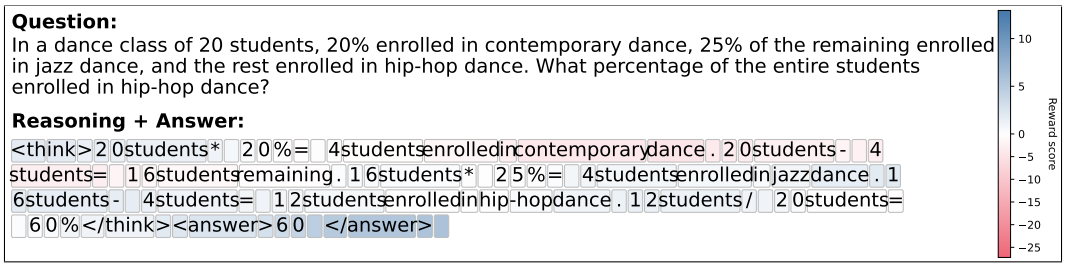

(a) Correct example 1

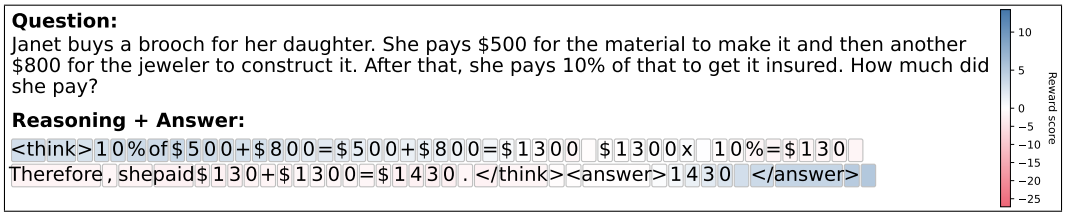

(b) Correct example 2

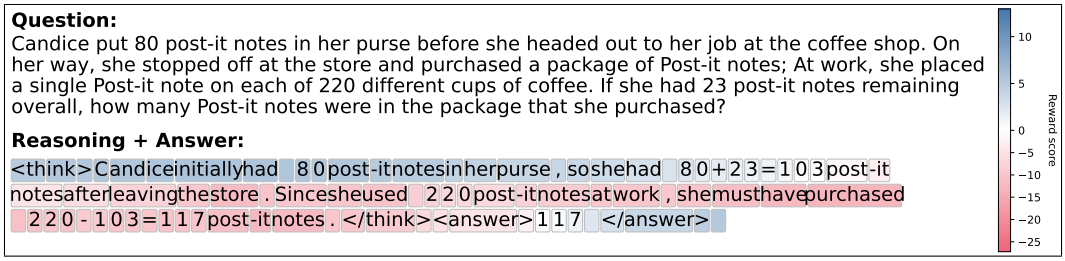

(c) Wrong example 1

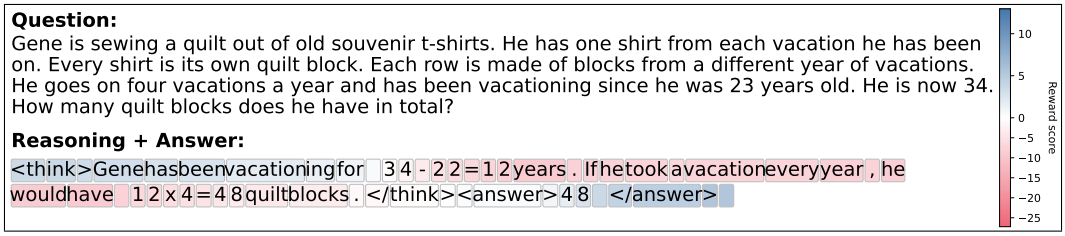

(d) Wrong example 2

Figure 14: **Dense reward illustrations for (Qwen2.5-3B-Instruct & Qwen2.5-1.5B-Instruct).** Two correct and two wrong examples of dense rewards ($\gamma = 0.9$). Correct cases show contiguous positive reward bands aligned with decisive reasoning, while wrong cases show inconsistent or negative signals.

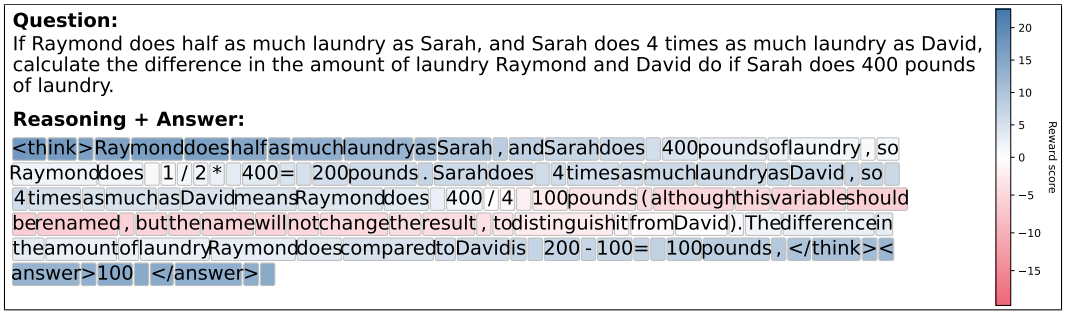

(a) Correct example 1

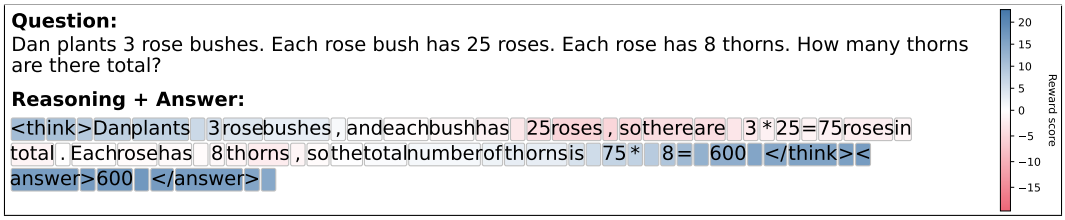

(b) Correct example 2

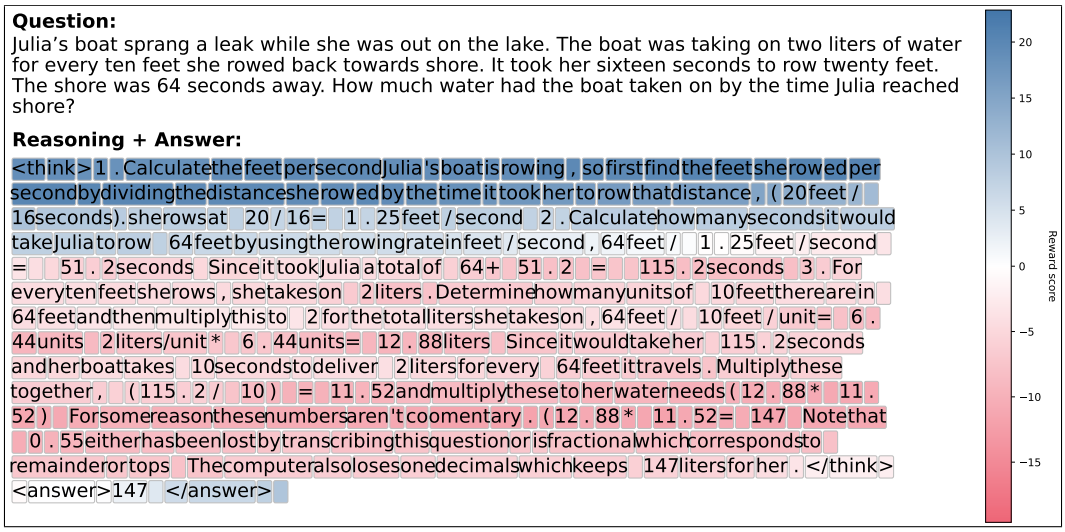

(c) Wrong example 1

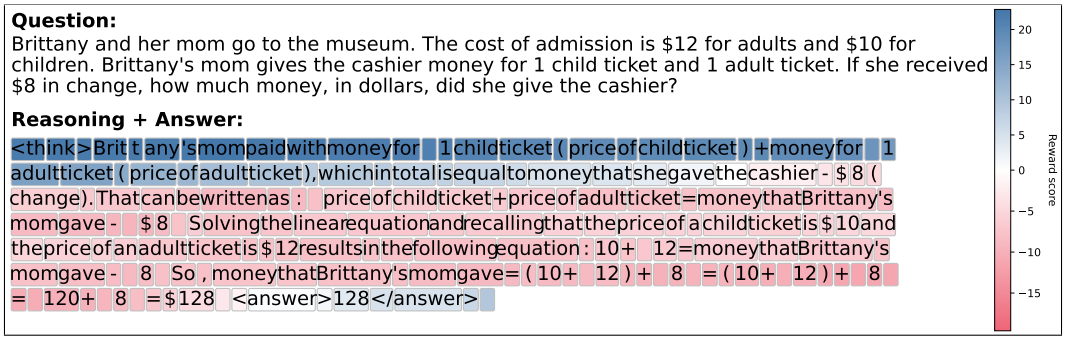

(d) Wrong example 2

Figure 15: **Dense reward illustrations for (Llama3.1-3B-Instruct & Llama3.1-1B-Instruct).** Two correct and two wrong examples of dense rewards ($\gamma = 0.9$). Correct cases show contiguous positive reward bands aligned with decisive reasoning, while wrong cases show inconsistent or negative signals.

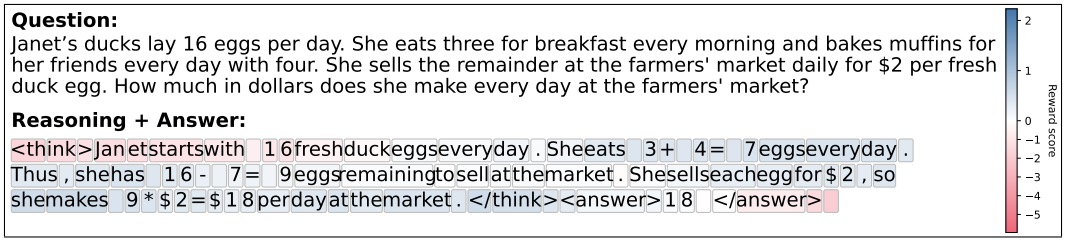

(a) Correct example 1

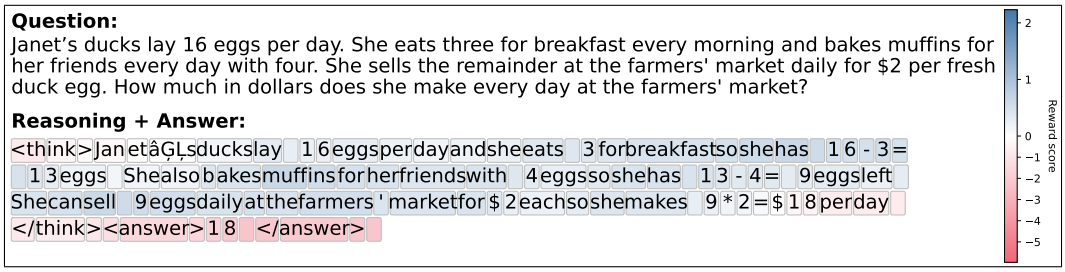

(b) Correct example 2

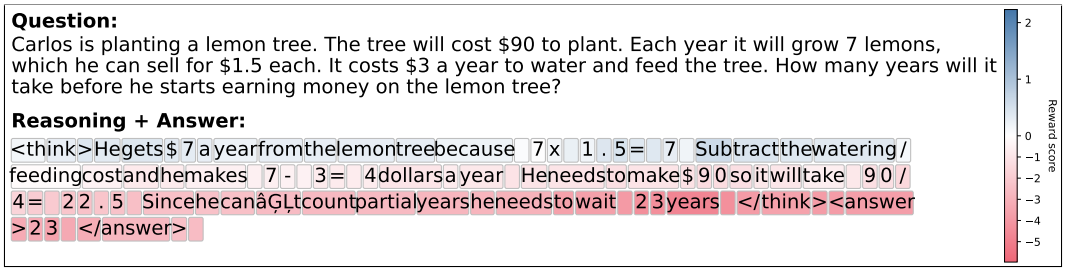

(c) Wrong example 1

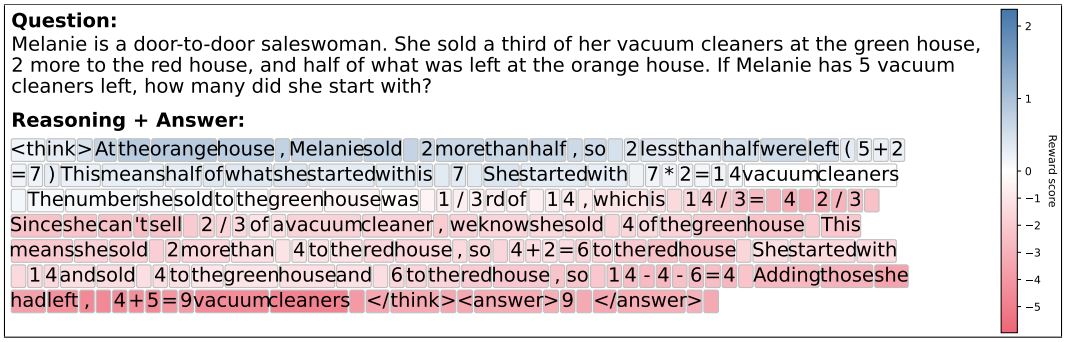

(d) Wrong example 2

Figure 16: **Dense reward illustrations for (Qwen2.5-7B-Instruct & Qwen2.5-1.5B-Instruct).** Two correct and two wrong examples of dense rewards ($\gamma = 0.9$). Correct cases show contiguous positive reward bands aligned with decisive reasoning, while wrong cases show inconsistent or negative signals.

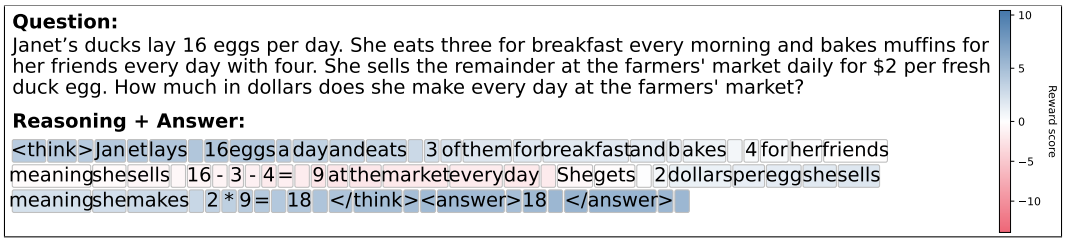

(a) Correct example 1

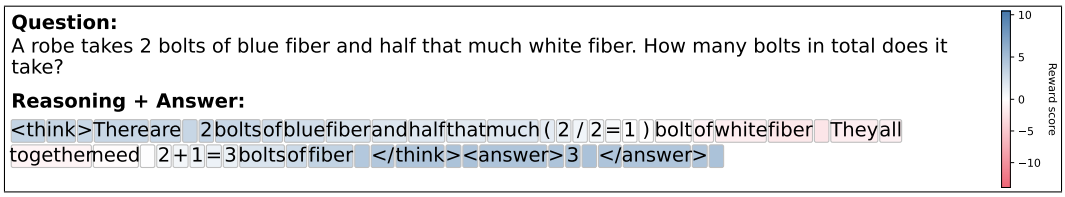

(b) Correct example 2

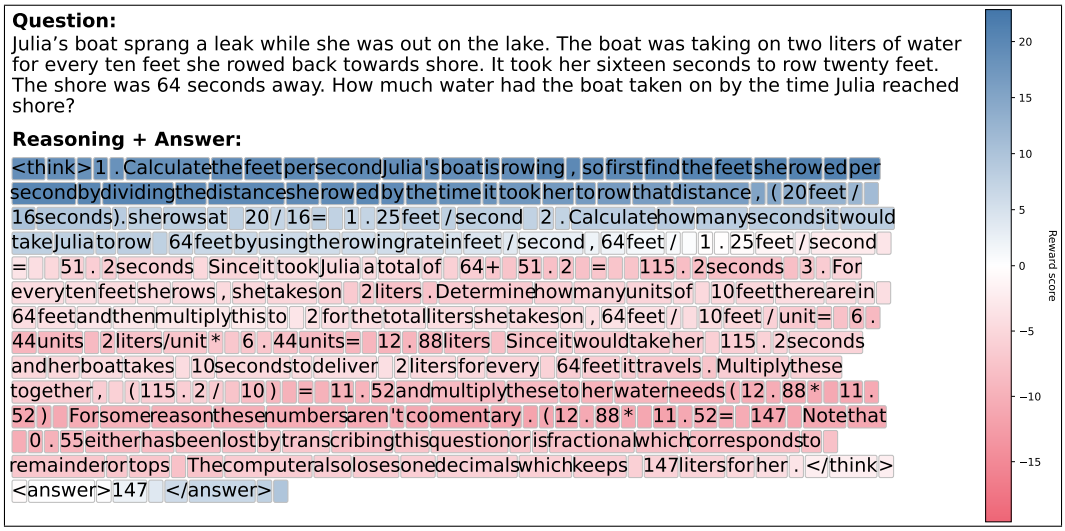

(c) Wrong example 1

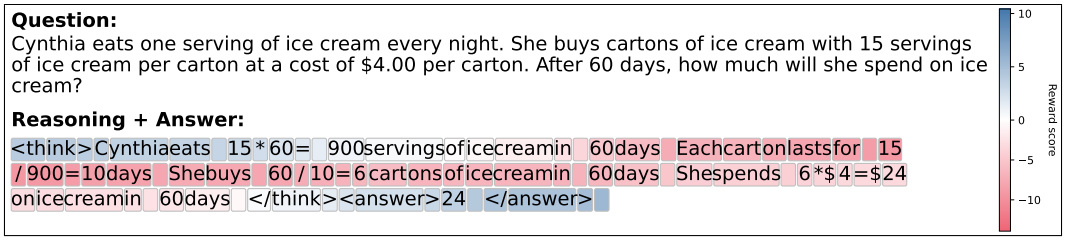

(d) Wrong example 2

Figure 17: **Dense reward illustrations for (Llama3.1-8B-Instruct & Llama3.1-1B-Instruct).** Two correct and two wrong examples of dense rewards ($\gamma = 0.9$). Correct cases show contiguous positive reward bands aligned with decisive reasoning, while wrong cases show inconsistent or negative signals.

C MEDICAL REASONING

To demonstrate the effectivness of the proposed method to extract a dense reasoning reward model, we extend our experiments to the MedReason (Wu et al., 2025), and more specifically to the MedQA (Jin et al., 2021) subset, consisting of US medical board exam questions, and MedMCQA (Pal et al., 2022) subset, comprising entrance exam questions from the Indian medical school curriculum. The dataset we use in our experiments consists of about 7'000 questions for training and 1'500 for evaluation. Moreover, the Wu et al. (2025) provides quality filtered medical reasoning traces constructed by strong language models (ChatGPT), which can be used for supervised fine-tuning, or in our case, adversarial inverse RL.

We train the same combination of models as with GSM8K and keep the hyperparameters; however, to speed up convergence, we first fine-tune the policy models on the reasoning chains to already have style-matching patterns with the expert demonstrations. Moreover, in this medical reasoning case, we do not introduce any corruption of correctness during adversarial training, as constructing such a function, compared to maths, is non-trivial and often requires a knowledge database or a more powerful language model. We leave this experiment as future work.

In the following subsections, we present the same experiments as previously demonstrated on the GSM8K dataset.

In subsection C.1, we analyse the training behaviour . Figure 18 shows the evolution of the learned reward and correctness accuracy on the MedReason benchmark across all policy–discriminator pairs. As on GSM8K, the evaluation reward broadly tracks the training reward and exhibits the characteristic non-monotonic dynamics of the adversarial game. However, the correctness curves are noisier and show improvement for the `Llama3` models, but `Qwen2.5-7B` even degrades. This indicates that, on the more specialised MedReason dataset, optimising the dense reasoning reward alone does not consistently translate into higher task accuracy, even though it remains a meaningful process-level signal.

We perform the reranking experiments in Subsection C.2.Figure 19 evaluates the learned reasoning reward as an inference-time assistant on MedReason across all policy–discriminator pairs. For each backbone, the distribution of mean discounted rewards for answer tokens is clearly shifted towards higher values on correct solutions, with large t-statistics ($p < 0.001$), indicating that the critic is calibrated to medical correctness rather than noise. Using these scores to rerank $N = 16$ sampled traces consistently improves pass@$k \mid N$ over random ranking across $k \in \{1, 3, 5, 10\}$, with the most significant gains at small k where selection is most constrained. Taken together, these results show that the same dense reward learned from expert traces can act as a useful decision aid at inference time, prioritising higher-quality clinical reasoning paths under a fixed sampling budget. For completeness we also report the pass@k metrics against verifiable outcomes (GRPO) and SFT in Table 2.

Figure 20 in Subsection 20 reports the correlation between our learned reasoning reward and the verifiable signals used in GRPO training on MedReason. Across all backbones, the reward correlates more strongly with verifiable style features, such as XML tag usage and strict formatting. Unlike our GSM8K experiments, here we do not introduce perturbations to expert demonstrations, so correctness varies less than stylistic features, and the critic naturally focuses on these more easily verifiable aspects of the traces, however, for the larger models, such as `Qwen2.5-7B` and `Llama3.1-8B` the correlation between discounted rewards and medical correctness is still larger than 0.20.

Figures 21–24 of Subsection C.4 provide qualitative heatmaps of token-level rewards for correct and incorrect MedReason solutions across all backbone pairs. In correct cases, the critic assigns a high reward to clinically salient steps. In contrast, in incorrect cases, it penalises spans of misleading reasoning and unsupported conclusions, potentially localising where the clinical argument breaks down.

C.1 Using the Learned Reward as a Training Signal

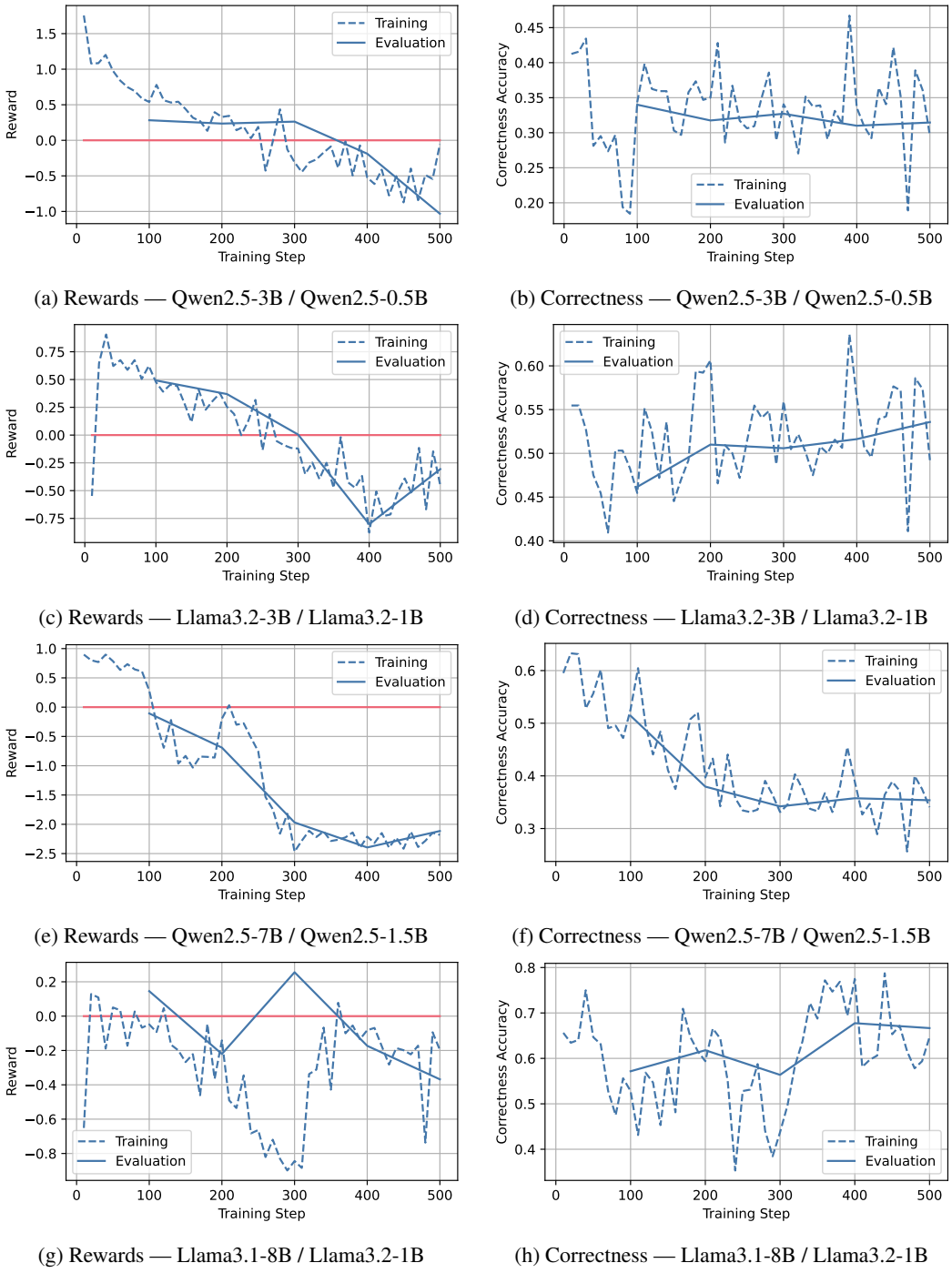

(a) Rewards — Qwen2.5-3B / Qwen2.5-0.5B

(b) Correctness — Qwen2.5-3B / Qwen2.5-0.5B

(c) Rewards — Llama3.2-3B / Llama3.2-1B

(d) Correctness — Llama3.2-3B / Llama3.2-1B

(e) Rewards — Qwen2.5-7B / Qwen2.5-1.5B

(f) Correctness — Qwen2.5-7B / Qwen2.5-1.5B

(g) Rewards — Llama3.1-8B / Llama3.2-1B

(h) Correctness — Llama3.1-8B / Llama3.2-1B

Figure 18: **Training behaviour of learned rewards and correctness across all MedReason model pairs.** Each row corresponds to one backbone pair, showing reward optimisation (left) and correctness over training (right).

> **Takeaway:** On MedReason, directly optimising the learned reasoning reward is noisier than on the GSM8K dataset. It seems to be working better for Llama family backbones.

C.2 Inference Time Assistance via Reward-guided Reranking

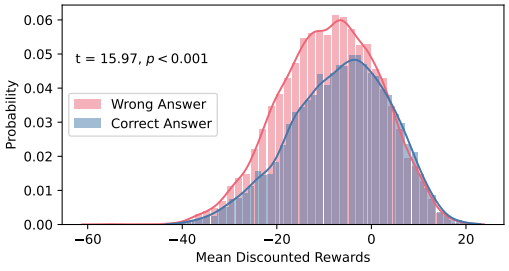

(a) Mean discounted rewards — Qwen2.5-3B / Qwen2.5-0.5B

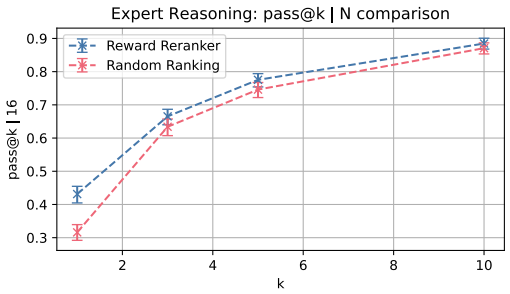

(b) Pass@k|N — Qwen2.5-3B / Qwen2.5-0.5B

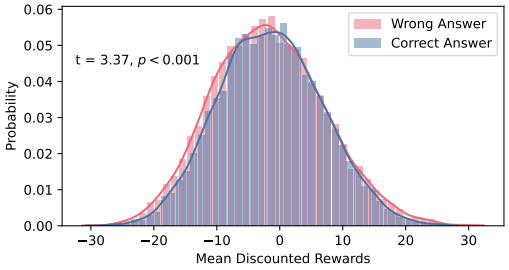

(c) Mean discounted rewards — Llama3.2-3B / Llama3.2-1B

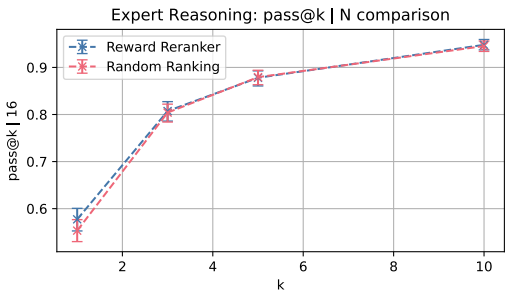

(d) Pass@k|N — Llama3.2-3B / Llama3.2-1B

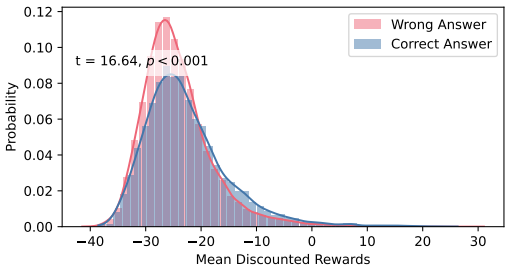

(e) Mean discounted rewards — Qwen2.5-7B / Qwen2.5-1.5B

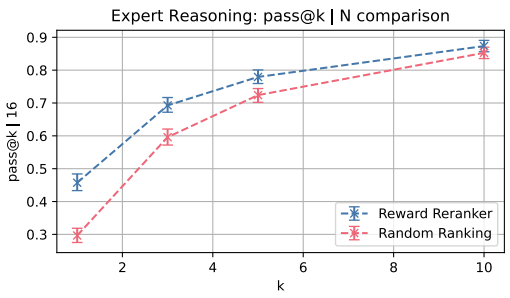

(f) Pass@k|N — Qwen2.5-7B / Qwen2.5-1.5B

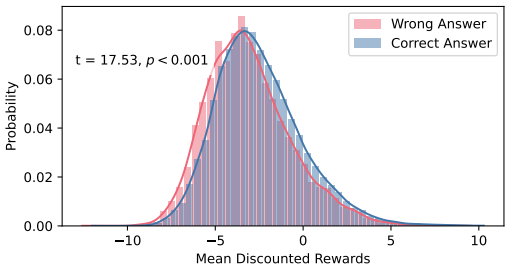

(g) Mean discounted rewards — Llama3.1-8B / Llama3.2-1B

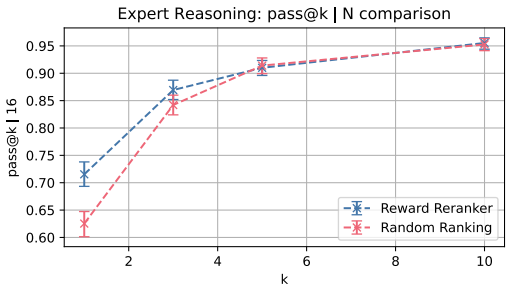

(h) Pass@k|N — Llama3.1-8B / Llama3.2-1B

Figure 19: **Benefit of the reasoning reward model across MedReason backbones.** Each row corresponds to a backbone pair, showing the distribution of mean discounted reasoning rewards (left) and validation Pass@k|N (right) for policies trained on the MedReason dataset

Takeaway: The same reward model is well-aligned with medical correctness and reliably boosts pass@k via reranking, making it an effective inference-time decision aid even when fine-tuning benefits are limited.

C.3 REWARD CORRELATION WITH STYLE AND CORRECTNESS

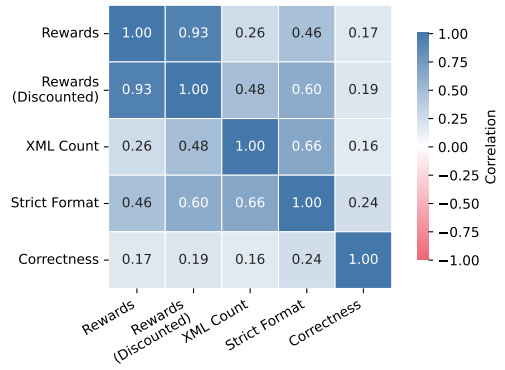

(a) (`Qwen2.5-3B-Instruct` - `Qwen2.5-0.5B-Instruct`)

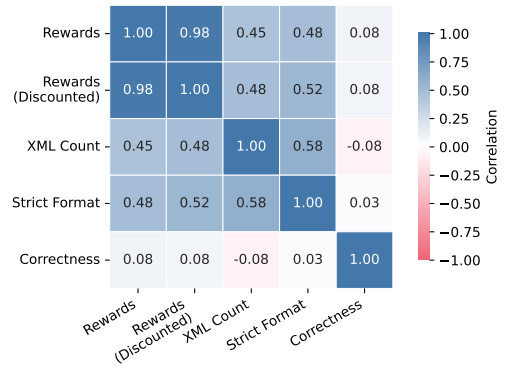

(b) (`Llama3.2-3B-Instruct` - `Llama3.2-1B-Instruct`)

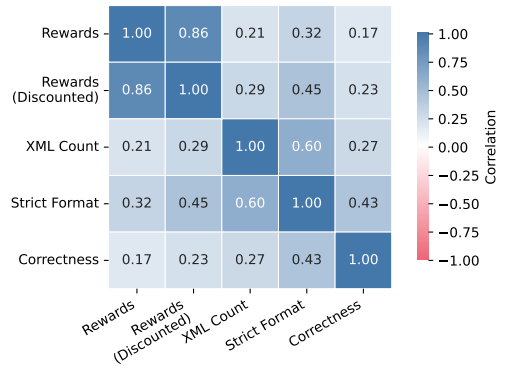

(c) (`Qwen2.5-7B-Instruct` - `Qwen2.5-1.5B-Instruct`)

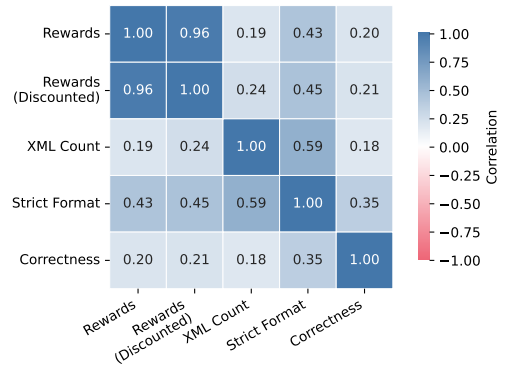

(d) (`Llama3.1-8B-Instruct` - `Llama3.2-1B-Instruct`)

Figure 20: **Correlation Matrix of Verifiable Rewards with Learned Reward.** Correlation between the mean rewards of the answer tokens and the various verifiable rewards used in GRPO training. We are especially interested in the correlation between correctness and the rewards.

> **Takeaway:** Without perturbing expert demonstrations, the learned reward on MedReason aligns more with style matching; however, with larger models like Llama3.1-8B and Qwen2.5-7B a strong positive correlation with the discounted reward is still measured.

C.4 INTERPRETABLE DENSE REWARDS AND LOCALISATION OF ERRORS

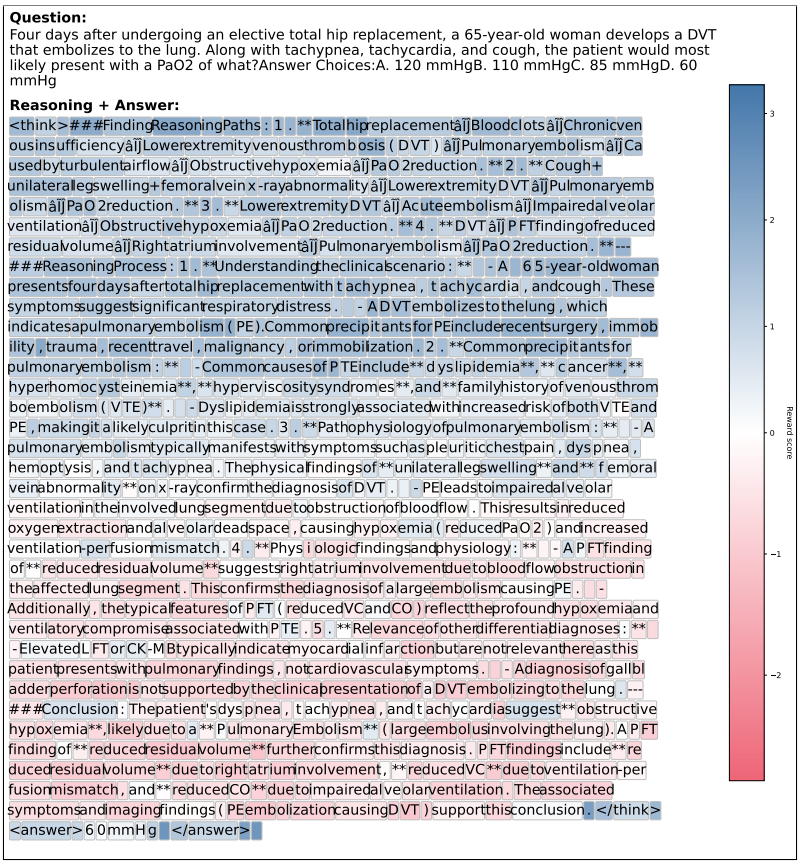

(a) Correct example 1

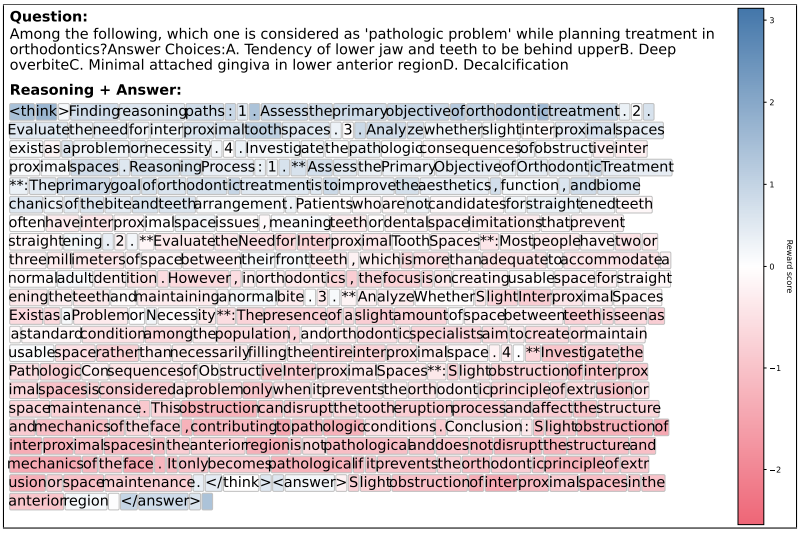

(b) Wrong example 1

Figure 21: **Dense reward illustrations for (Qwen2.5-3B-Instruct & Qwen2.5-0.5B-Instruct).** Two correct and two wrong examples of dense rewards on MedReasoning.

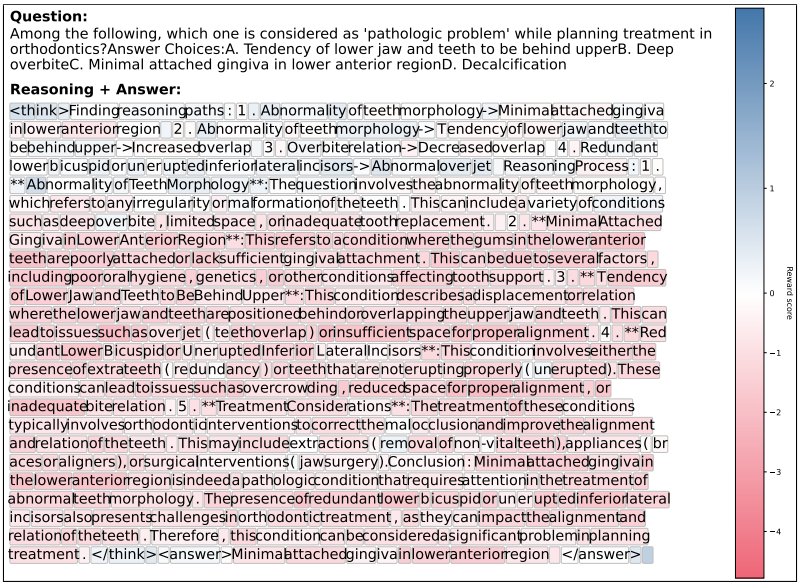

(a) Correct example 1

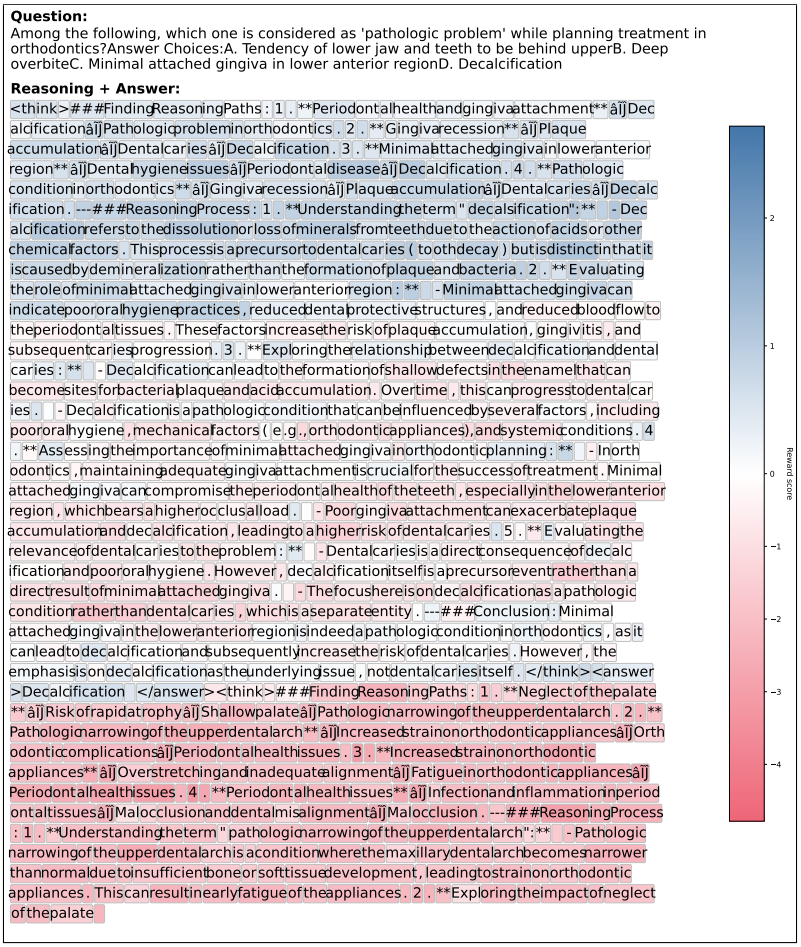

(b) Wrong example 1

Figure 22: **Dense reward illustrations for (Llama3.2-3B-Instruct & Llama3.2-1.5B-Instruct).** Two correct and two wrong examples of dense rewards on MedReasoning.

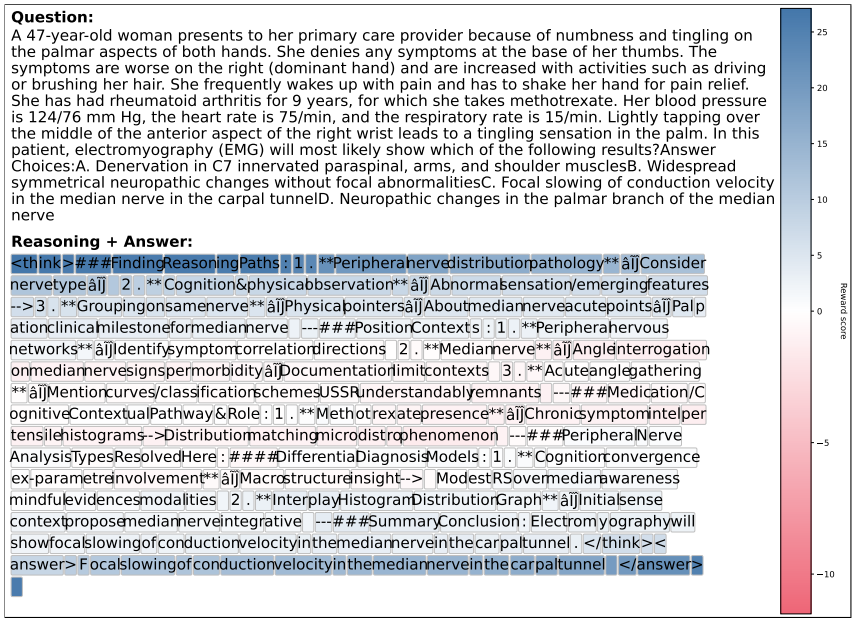

(a) Correct example 1

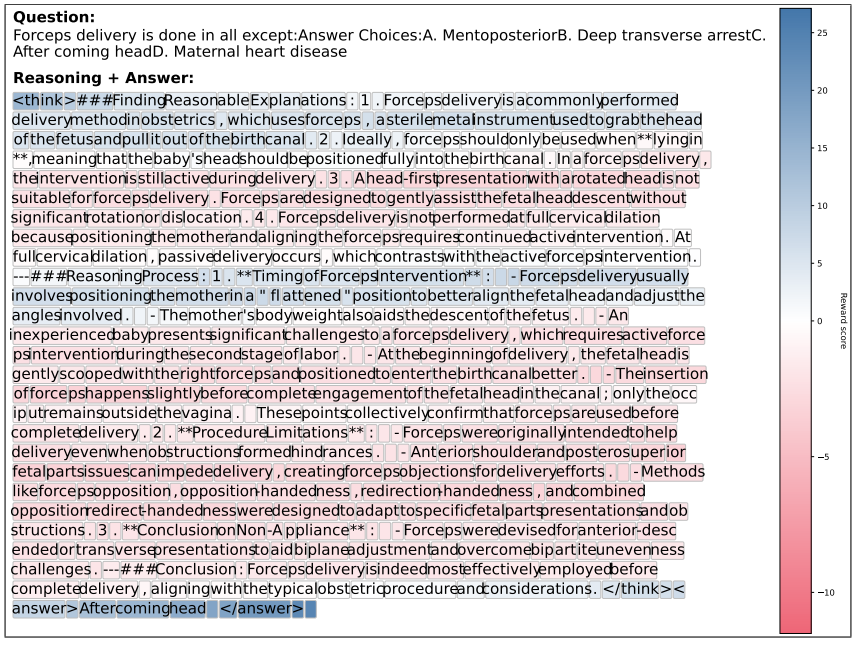

(b) Wrong example 1

Figure 23: **Dense reward illustrations for (Qwen2.5-7B-Instruct & Qwen2.5-1.5B-Instruct).** Two correct and two wrong examples of dense rewards on MedReasoning.

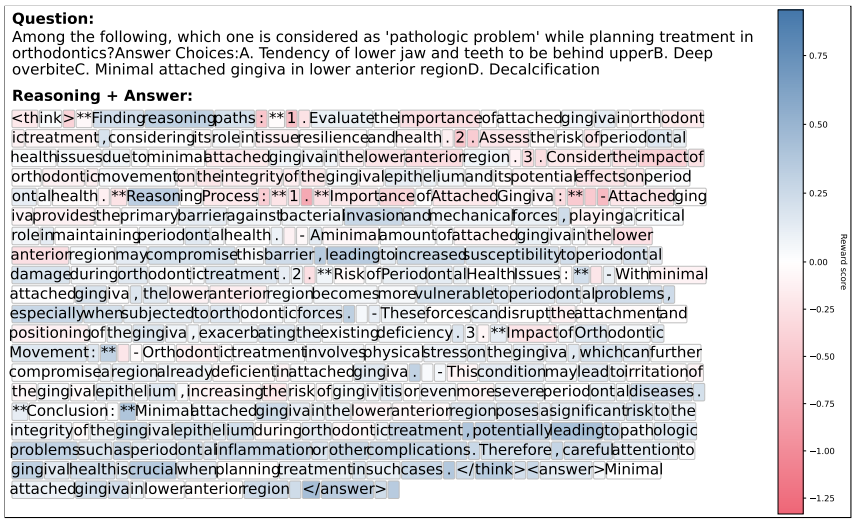

(a) Correct example 1

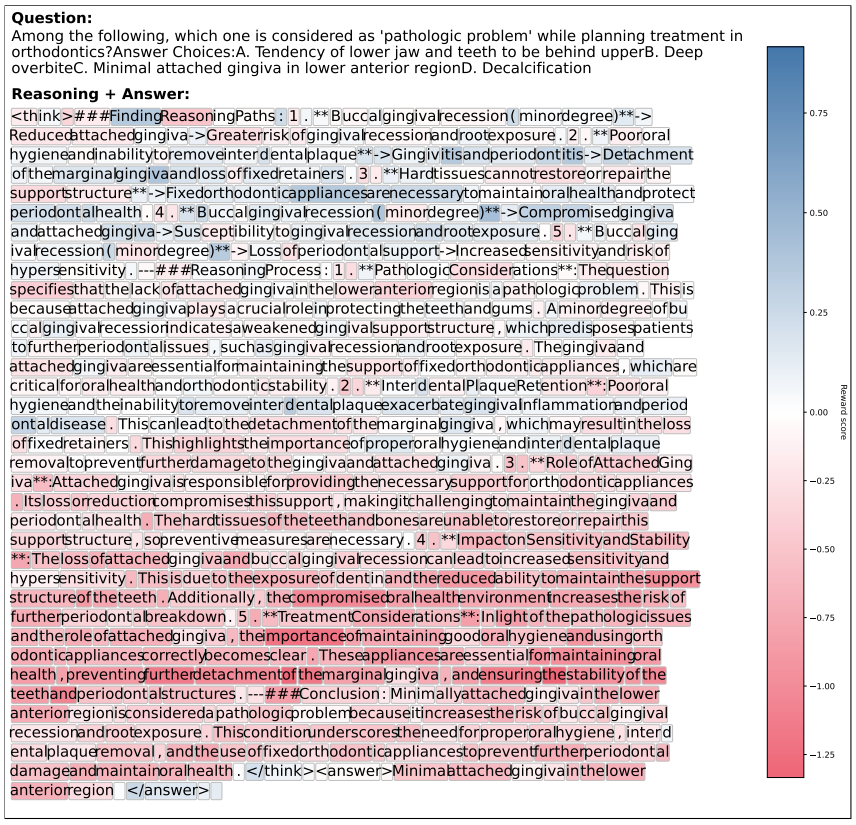

(b) Wrong example 1

Figure 24: **Dense reward illustrations for (Llama3.1-8B-Instruct & Llama3.2-1B-Instruct).** Two correct and two wrong examples of dense rewards on MedReasoning.

D Additional Experiments

D.1 Comaprison against Verifiable Rewards and Supervised Finetuning

We benchmark predictive performance against two references. The first is supervised fine-tuning on reasoning traces (SFT). The second is GRPO, which uses a verifiable outcome reward at the final answer and therefore acts as an empirical upper bound. For each backbone, we evaluate the same prompt set and report pass@1, pass@3, pass@5, and pass@10, along with their corresponding confidence intervals. Our method, labelled *Expert Reasoning (ours)*, uses the learned dense reward for training the policy; at test time we decode with the same settings as the baselines.

Table 2 shows consistent trends. GRPO traces the strongest curve across all backbones, as expected from access to verifiable outcomes. Our approach is frequently competitive with SFT, and on Qwen2.5-7B it exceeds SFT at all reported pass@k, including pass@1. For GS8MK on Llama3-3B and 8B, as well as on Qwen2.5-3B, our method trails SFT at pass@1 but narrows the gap as k increases. These results quantify the current trade-off between joint optimisation with a learned process reward and outcome supervised training.

The MedReason portion of Table 2, our Expert Reasoning policy remains competitive with SFT: on Llama3.2-3B, the two methods are essentially indistinguishable across all reported pass@k, and on Qwen2.5-7B, our approach slightly improves pass@1 while staying within a few points of SFT at larger k. For Qwen2.5-3B and Llama3.1-8B our method lags SFT in raw pass@k, but the gap shrinks as k increases. Taken together, these results show that on MedReason, our learned dense process reward yields policies with comparable final-answer accuracy to outcome-supervised SFT, while providing the additional benefits of a reusable, step-wise reward model over reasoning traces.

Backbone	Algorithm	pass@1	pass@3	pass@5	pass@10
Dataset: GSM8K					
P : Qwen-2.5-3B-Instruct D: Qwen-2.5-0.5B-Instruct	Outcome Sup.	**0.80** [0.78, 0.82]	**0.90** [0.89, 0.92]	**0.93** [0.91, 0.94]	**0.95** [0.93, 0.96]
	Exp. Reas. (ours)	0.51 [0.49, 0.53]	0.72 [0.71, 0.74]	0.80 [0.78, 0.81]	0.87 [0.85, 0.88]
	SFT	0.54 [0.53, 0.56]	0.76 [0.75, 0.78]	0.83 [0.81, 0.85]	0.90 [0.88, 0.91]
P: Llama3.2-3B-Instruct D: Llama3.2-1B-Instruct	Outcome Sup.	**0.57** [0.55, 0.59]	**0.78** [0.77, 0.80]	**0.85** [0.83, 0.86]	**0.91** [0.89, 0.92]
	Exp. Reas. (ours)	0.32 [0.30, 0.33]	0.53 [0.51, 0.55]	0.63 [0.61, 0.65]	0.75 [0.73, 0.77]
	SFT	0.55 [0.53, 0.57]	0.76 [0.75, 0.78]	0.83 [0.82, 0.85]	0.89 [0.88, 0.91]
P: Qwen-2.5-7B-Instruct D: Qwen-2.5-1.5B-Instruct	Outcome Sup.	**0.88** [0.87, 0.90]	**0.94** [0.93, 0.95]	**0.95** [0.94, 0.96]	**0.96** [0.95, 0.97]
	Exp. Reas. (ours)	0.71 [0.69, 0.73]	0.88 [0.87, 0.90]	0.92 [0.91, 0.93]	**0.95** [0.94, 0.96]
	SFT	0.67 [0.66, 0.69]	0.87 [0.85, 0.88]	0.91 [0.90, 0.93]	0.95 [0.94, 0.96]
P: Llama3.1-8B-Instruct D: Llama3.2-1B-Instruct	Outcome Sup.	**0.73** [0.71, 0.74]	**0.88** [0.86, 0.89]	**0.91** [0.90, 0.93]	**0.94** [0.93, 0.95]
	Exp. Reas. (ours)	0.49 [0.47, 0.51]	0.73 [0.71, 0.75]	0.80 [0.79, 0.82]	0.88 [0.86, 0.89]
	SFT	0.55 [0.53, 0.56]	0.79 [0.78, 0.81]	0.86 [0.84, 0.87]	0.91 [0.90, 0.93]
Dataset: MedReason					
P : Qwen-2.5-3B-Instruct D: Qwen-2.5-0.5B-Instruct	Outcome Sup.	**0.54** [0.52, 0.55]	0.69 [0.67, 0.71]	0.75 [0.73, 0.77]	0.81 [0.80, 0.83]
	Exp. Reas. (ours)	0.37 [0.36, 0.38]	0.64 [0.63, 0.66]	0.76 [0.74, 0.77]	0.87 [0.86, 0.88]
	SFT	0.44 [0.42, 0.45]	**0.70** [0.69, 0.72]	**0.80** [0.79, 0.82]	**0.90** [0.89, 0.91]
P: Llama3.2-3B-Instruct D: Llama3.2-1B-Instruct	Outcome Sup.	0.29 [0.28, 0.30]	0.54 [0.53, 0.56]	0.66 [0.64, 0.68]	0.79 [0.77, 0.80]
	Exp. Reas. (ours)	**0.56** [0.55, 0.58]	**0.81** [0.80, 0.82]	**0.88** [0.87, 0.89]	**0.94** [0.93, 0.95]
	SFT	**0.56** [0.55, 0.57]	**0.81** [0.80, 0.82]	**0.88** [0.87, 0.90]	**0.94** [0.93, 0.95]
P: Qwen-2.5-7B-Instruct D: Qwen-2.5-1.5B-Instruct	Outcome Sup.	0.64 [0.63, 0.66]	0.85 [0.84, 0.86]	0.90 [0.89, 0.92]	0.95 [0.94, 0.96]
	Exp. Reas. (ours)	**0.66** [0.65, 0.68]	**0.86** [0.85, 0.87]	0.91 [0.90, 0.92]	0.95 [0.94, 0.96]
	SFT	0.64 [0.62, 0.65]	**0.86** [0.85, 0.88]	**0.92** [0.91, 0.93]	**0.96** [0.95, 0.97]
P: Llama3.1-8B-Instruct D: Llama3.2-1B-Instruct	Outcome Sup.	**0.66** [0.64, 0.68]	**0.80** [0.79, 0.82]	0.85 [0.83, 0.86]	0.90 [0.88, 0.91]
	Exp. Reas. (ours)	0.35 [0.34, 0.36]	0.62 [0.61, 0.64]	0.73 [0.72, 0.75]	0.85 [0.84, 0.87]
	SFT	0.56 [0.54, 0.57]	0.79 [0.77, 0.80]	**0.86** [0.85, 0.87]	**0.93** [0.92, 0.94]

Table 2: Results (mean ± 95%-CI) for different algorithms across GSM8K and MedReason.

Takeaway: Outcome reward RL with verifiable signals remains the empirical upper bound for GSM8K. The learned process reward is often close to SFT and can exceed it on Qwen-2.5 7B, while trailing on some other settings, especially at pass@1. Closing this gap without losing the training, inference, and diagnostic benefits of the dense reward is a concrete direction for future work.

D.2 CHANGING DISCRIMINATOR BACKBONES

We study the effect of the discriminator backbone size and specialisation for a fixed `Qwen2.5-7B Instruct` policy. Table 3 shows that a larger general-purpose discriminator (`Qwen2.5-1.5B-Instruct`) attains the strongest performance across pass@k, with the largest gains at low k. The smaller `0.5B` variant trails at pass@1 but approaches parity by pass@10. A maths specialised `1.5B` discriminator does not outperform the general purpose counterpart.

Discriminator	pass@1	pass@3	pass@5	pass@10
Qwen 2.5 0.5B Instruct	0.66 [0.65, 0.68]	0.86 [0.84, 0.87]	0.90 [0.89, 0.92]	**0.95** [0.93, 0.96]
Qwen 2.5 1.5B Instruct	**0.71** [0.69, 0.73]	**0.88** [0.87, 0.90]	**0.92** [0.91, 0.93]	**0.95** [0.94, 0.96]
Qwen 2.5 Math 1.5B Instruct	0.65 [0.64, 0.67]	0.85 [0.84, 0.87]	0.90 [0.89, 0.92]	0.94 [0.93, 0.95]

Table 3: Performance (mean with confidence intervals) for different discriminator backbones with a fixed `Qwen2.5-7B-Instruct` policy.

> **Takeaway:** A larger general-purpose discriminator improves accuracy, especially at pass@1. A maths specialised discriminator of the same size does not confer additional gains in this setting.

D.3 Training without Perturbation

We study the impact of introducing perturbed traces during training, where we flip operator signs, corrupt numeric literals, and swap the final answer with a previous intermediate quantity. These perturbations are applied to both expert and policy traces and are labelled as non expert. Table 4 and Figure 25 compare training *with* versus *without* perturbations for the `Llama3.1-8B-Instruct` policy and `Llama3.2-1B-Instruct` discriminator.

Negative Perturbation	pass@1	pass@3	pass@5	pass@10
✗	0.31 [0.29, 0.32]	0.56 [0.54, 0.57]	0.67 [0.65, 0.69]	0.79 [0.77, 0.80]
✓	**0.49** [0.47, 0.51]	**0.73** [0.71, 0.75]	**0.80** [0.79, 0.82]	**0.88** [0.86, 0.89]

Table 4: Results (mean ± CI) when using negative perturbation during training vs. without it for the (`Llama3.2-3B-Instruct - Llama3.2-1B-Instruct`) combination.

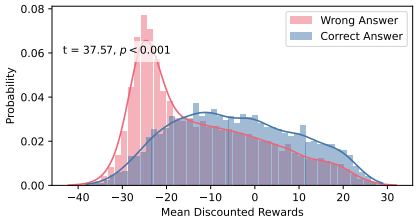

(a) Reward distribution **without** negative perturbations

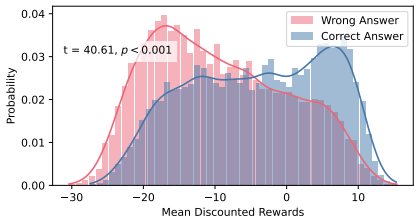

(b) Reward distribution **with** negative perturbations

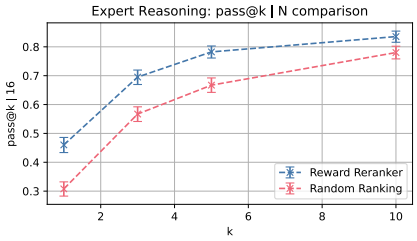

(c) Reward reranking **without** negative perturbations

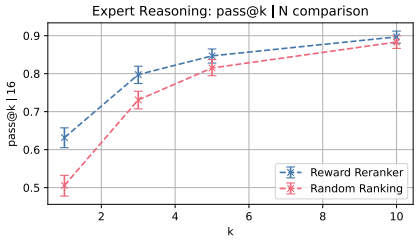

(d) Reward reranking **with** negative perturbations

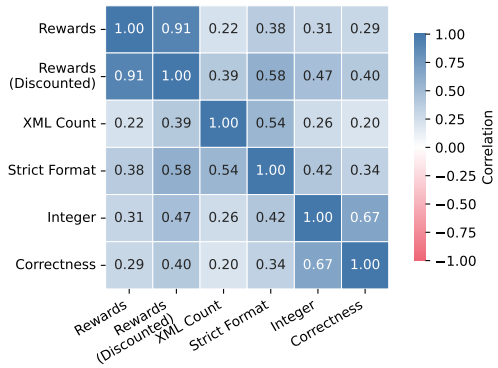

(e) Correlation to verifiable rewards **without** negative perturbations

(f) Correlation to verifiable rewards **with** negative perturbations

Figure 25: **Distribution and Correlation of Learned Rewards.** For the (`Llama3.1-8B-Instruct - Llama3.2-1B-Instruct`) combination, we run training with and without negative perturbations.

D.4 WASSERSTEIN GAN DISCRIMINATOR LOSS

We replace the binary cross-entropy objective for the discriminator with a Wasserstein GAN loss and repeat training across backbones. Table 5 and Figures 26, 27, 28, and 29 report predictive performance, reward distributions, and pass@$k \mid N$ reranking curves. Across settings, the Wasserstein variant yields lower pass@k than binary cross entropy, with the largest drop at pass@1. The learned reward exhibits heavy tails and weaker separation between correct and incorrect answers, which in turn reduces the benefit of reward-guided reranking.

Backbone	Discriminator Loss	pass@1	pass@3	pass@5	pass@10
P : Qwen-2.5-3B-Instruct	Binary Cross Entropy	0.51 [0.49, 0.53]	0.72 [0.71, 0.74]	0.80 [0.78, 0.81]	0.87 [0.85, 0.88]
D: Qwen-2.5-0.5B-Instruct	Wasserstein GAN	**0.58** [0.56, 0.59]	**0.75** [0.73, 0.77]	**0.81** [0.80, 0.83]	**0.88** [0.86, 0.89]
P: Llama3.1-3B-Instruct	Binary Cross Entropy	**0.32** [0.30, 0.33]	**0.53** [0.51, 0.55]	**0.63** [0.61, 0.65]	**0.75** [0.73, 0.77]
D: Llama3.2-1B-Instruct	Wasserstein GAN	0.17 [0.16, 0.18]	0.39 [0.37, 0.40]	0.51 [0.49, 0.53]	0.67 [0.65, 0.69]
P: Qwen-2.5-7B-Instruct	Binary Cross Entropy	**0.71** [0.69, 0.73]	**0.88** [0.87, 0.90]	**0.92** [0.91, 0.93]	**0.95** [0.94, 0.96]
D: Qwen-2.5-1.5B-Instruct	Wasserstein GAN	0.65 [0.64, 0.67]	0.85 [0.84, 0.86]	0.90 [0.89, 0.91]	0.94 [0.93, 0.95]
P: Llama3.1-8B-Instruct	Binary Cross Entropy	**0.49** [0.47, 0.51]	**0.73** [0.71, 0.75]	**0.80** [0.79, 0.82]	**0.88** [0.86, 0.89]
D: Llama3.2-1B-Instruct	Wasserstein GAN	0.33 [0.32, 0.34]	0.59 [0.57, 0.61]	0.70 [0.68, 0.72]	0.81 [0.80, 0.83]

Table 5: Results (mean $\pm$ CI) for binary cross-entropy and Wasserstein GAN loss for the discriminator.

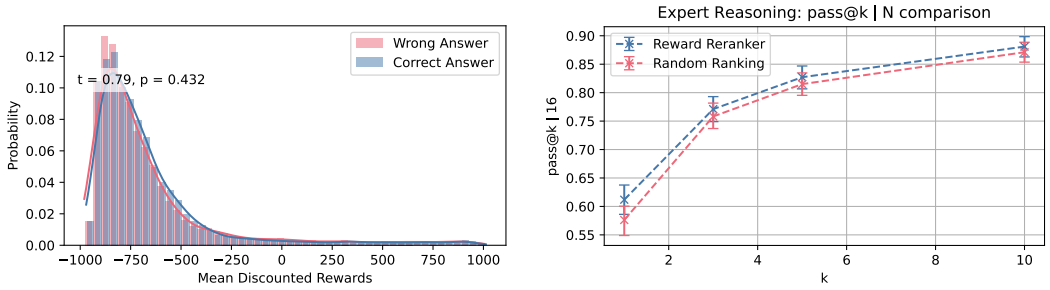

(a) Distribution of mean discounted (b) Pass@k|N

Figure 26: **Benefit of Reasoning Reward Model.** This is for the (`Qwen2.5-3B-Instruct` - `Qwen2.5-0.5B-Instruct`) combination using the Wasserstein loss for the discriminator.

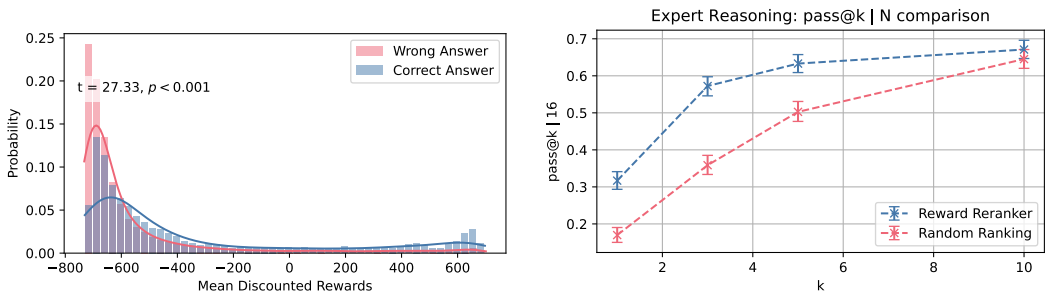

(a) Distribution of mean discounted rewards (b) Pass@k|N

Figure 27: **Benefit of Reasoning Reward Model.** This is for the (`Llama3.2-3B-Instruct` - `Llama3.2-1B-Instruct`) combination using the Wasserstein loss for the discriminator.

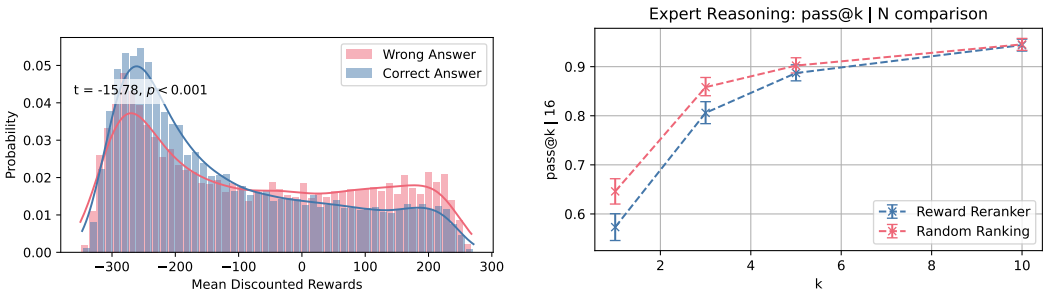

(a) Distribution of mean discounted rewards (b) Pass@k|N

Figure 28: **Benefit of Reasoning Reward Model.** This is for the (`Qwen2.5-7B-Instruct` - `Qwen2.5-1.5B-Instruct`) combination using the Wasserstein loss for the discriminator.

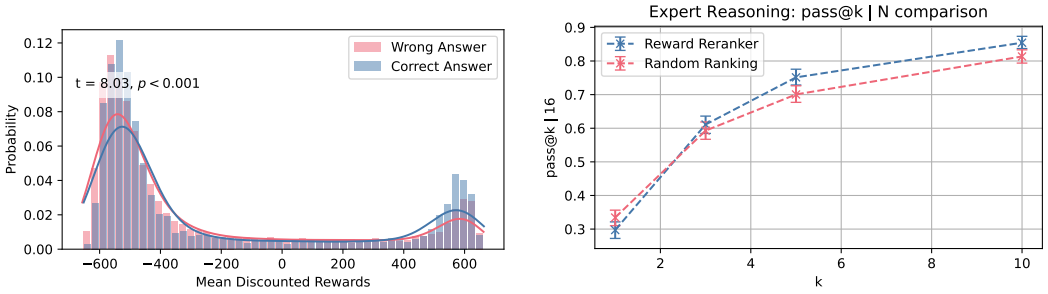

(a) Distribution of mean discounted rewards (b) Pass@k|N

Figure 29: **Benefit of Reasoning Reward Model.** This is for the (`Llama3.1-8B-Instruct` - `Llama3.2-1B-Instruct`) combination using the Wasserstein loss for the discriminator.

Takeaway: Binary cross-entropy is a more stable and effective discriminator objective than Wasserstein GAN in our setting. Wasserstein training produces poorly calibrated rewards, weaker class separation, and lower predictive performance.

D.5 Dense vs. Sparse Reward Models

In this experiment, we aim to evaluate the predictive performance of using a sequence classifier as a discriminator, which effectively mimics an outcome-based reward model rather than a dense, token-level reasoning reward. Note that this will come at the cost of not having a dense reward, which can be helpful for diagnostics and error-localisation tools. In Table 6 we report the results, and in three out of the four cases, the sparse reward model outperforms the dense reward model in predictive performance. We believe this is to be expected, as classifying a whole sequence originating from a completed sequence from an expert or a policy is simpler than classifying a partial, incomplete sequence.

Backbone	Dense vs. Sparse	pass@1	pass@3	pass@5	pass@10
P : Qwen-2.5-3B-Instruct	Dense	0.51 [0.49, 0.53]	0.72 [0.71, 0.74]	0.80 [0.78, 0.81]	0.87 [0.85, 0.88]
D: Qwen-2.5-0.5B-Instruct	Sparse	**0.57** [0.56, 0.59]	**0.78** [0.76, 0.80]	**0.84** [0.83, 0.86]	**0.90** [0.89, 0.92]
P: Llama3.1-3B-Instruct	Dense	0.32 [0.30, 0.33]	0.53 [0.51, 0.55]	0.63 [0.61, 0.65]	0.75 [0.73, 0.77]
D: Llama3.2-1B-Instruct	Sparse	**0.46** [0.44, 0.48]	**0.69** [0.68, 0.71]	**0.78** [0.76, 0.79]	**0.86** [0.84, 0.87]
P: Qwen-2.5-7B-Instruct	Dense	**0.71** [0.69, 0.73]	**0.88** [0.87, 0.90]	**0.92** [0.91, 0.93]	**0.95** [0.94, 0.96]
D: Qwen-2.5-1.5B-Instruct	Sparse	0.65 [0.64, 0.67]	0.85 [0.84, 0.86]	0.90 [0.89, 0.91]	0.94 [0.93, 0.95]
P: Llama3.1-8B-Instruct	Dense	0.49 [0.47, 0.51]	0.73 [0.71, 0.75]	0.80 [0.79, 0.82]	0.88 [0.86, 0.89]
D: Llama3.2-1B-Instruct	Sparse	**0.54** [0.52, 0.56]	**0.76** [0.74, 0.78]	**0.83** [0.81, 0.84]	**0.89** [0.87, 0.90]

Table 6: Results (mean $\pm$ CI) for dense and sparse (outcome) reward models. For the outcome reward models, we use a sequence classifier, rather than a token classifier.

> **Takeaway:** We observe that for three out of four cases, using an outcome reward model critic will lead to improved results over using a token-level reward model. However, this comes at the cost of not being able to create a dense reward of the reasoning, which is helpful to localise errors.

D.6 Normalised vs. Unnormalised Reward Models

In this section, we are interested in observing the effect of normalising the rewards before feeding them into the GRPO algorithm. We report our results in Table 7 and observe that, with the Llama models, the learning algorithm has collapsed. In all cases, the normalised rewards outperform the unnormalised approach. We believe this to be expected, as normalising with a baseline in PPO and GRPO helps reduce the variance in the reward signals.

Backbone	Normalised vs. Unnormalised	pass@1	pass@3	pass@5	pass@10
P : Qwen-2.5-3B-Instruct	Normalised	**0.51** [0.49, 0.53]	**0.72** [0.71, 0.74]	**0.80** [0.78, 0.81]	**0.87** [0.85, 0.88]
D: Qwen-2.5-0.5B-Instruct	Unnormalised	0.50 [0.48, 0.52]	0.71 [0.70, 0.73]	0.79 [0.77, 0.81]	0.86 [0.84, 0.88]
P: Llama3.1-3B-Instruct	Normalised	**0.32** [0.30, 0.33]	**0.53** [0.51, 0.55]	**0.63** [0.61, 0.65]	**0.75** [0.73, 0.77]
D: Llama3.2-1B-Instruct	Unnormalised	0.00 [0.00, 0.00]	0.00 [0.00, 0.00]	0.00 [0.00, 0.00]	0.00 [0.00, 0.00]
P: Qwen-2.5-7B-Instruct	Normalised	**0.71** [0.69, 0.73]	**0.88** [0.87, 0.90]	**0.92** [0.91, 0.93]	**0.95** [0.94, 0.96]
D: Qwen-2.5-1.5B-Instruct	Unnormalised	0.36 [0.34, 0.37]	0.63 [0.61, 0.64]	0.73 [0.71, 0.75]	0.83 [0.82, 0.85]
P: Llama3.1-8B-Instruct	Normalised	**0.49** [0.47, 0.51]	**0.73** [0.71, 0.75]	**0.80** [0.79, 0.82]	**0.88** [0.86, 0.89]
D: Llama3.2-1B-Instruct	Unnormalised	0.00 [0.00, 0.00]	0.00 [0.00, 0.00]	0.00 [0.00, 0.00]	0.00 [0.00, 0.00]

Table 7: Results (mean $\pm$ CI) for normalised and unnormalised dense reward models.

Takeaway: We observe that normalisation of the rewards is of key importance, as this stabilises the rewards in the GRPO algorithm. Not applying it can lead to model collapse, depending on the model family.

D.7 Effect of Errors in Expert Demonstrations

With this experiment, we are interested in analysing the effect of errors in the expert dataset. To this end, we corrupt the expert demonstrations on GSM8K with error rates of $\{0\%, 10\%, 25\%\}$ by randomly exchanging mathematical operators, perturbing intermediate numbers in the reasoning, and changing the answer values. We report our results in Table 8 and observe that corrupting the expert traces can have a strong, but model-dependent, effect on performance. For Qwen-2.5-3B and Llama3.1-8B, injecting only 10% errors in the expert demonstrations already leads to a significant drop in pass@1 (from 0.51 to 0.16 and from 0.49 to 0.07, respectively), and performance almost collapses at a 25% error rate. By contrast, the larger Qwen-2.5-7B backbone is remarkably robust: its pass@1 decreases only slightly from 0.71 to 0.68 when 25% of reasoning steps are corrupted. Interestingly, the Llama3.1-3B configuration shows non-monotonic behaviour: while 10% corruption hurts performance, a 25% error rate actually improves pass@1 to 0.45, surpassing the clean baseline, suggesting that in some cases noisy demonstrations may act as hard negatives that sharpen the learned reward.

Backbone	Expert Error Rate	pass@1	pass@3	pass@5	pass@10
P : Qwen-2.5-3B-Instruct D: Qwen-2.5-0.5B-Instruct	0%	**0.51** [0.49, 0.53]	**0.72** [0.71, 0.74]	**0.80** [0.78, 0.81]	**0.87** [0.85, 0.88]
	10%	0.16 [0.15, 0.17]	0.36 [0.34, 0.37]	0.48 [0.46, 0.50]	0.65 [0.62, 0.67]
	25%	0.00 [0.00, 0.00]	0.00 [0.00, 0.00]	0.00 [0.00, 0.00]	0.00 [0.00, 0.00]
P: Llama3.1-3B-Instruct D: Llama3.2-1B-Instruct	0%	0.32 [0.30, 0.33]	0.53 [0.51, 0.55]	0.63 [0.61, 0.65]	0.75 [0.73, 0.77]
	10%	0.12 [0.11, 0.13]	0.28 [0.27, 0.30]	0.39 [0.37, 0.41]	0.54 [0.52, 0.56]
	25%	**0.45** [0.43, 0.47]	**0.69** [0.67, 0.70]	**0.77** [0.75, 0.79]	**0.85** [0.84, 0.87]
P: Qwen-2.5-7B-Instruct D: Qwen-2.5-1.5B-Instruct	0%	**0.71** [0.69, 0.73]	**0.88** [0.87, 0.90]	**0.92** [0.91, 0.93]	**0.95** [0.94, 0.96]
	10%	0.70 [0.68, 0.71]	0.87 [0.86, 0.89]	0.91 [0.90, 0.92]	0.94 [0.93, 0.95]
	25%	0.68 [0.66, 0.70]	0.87 [0.85, 0.88]	0.91 [0.90, 0.92]	0.95 [0.94, 0.96]
P: Llama3.1-8B-Instruct D: Llama3.2-1B-Instruct	0%	**0.49** [0.47, 0.51]	**0.73** [0.71, 0.75]	**0.80** [0.79, 0.82]	**0.88** [0.86, 0.89]
	10%	0.07 [0.07, 0.08]	0.19 [0.18, 0.20]	0.28 [0.27, 0.30]	0.45 [0.43, 0.47]
	25%	0.03 [0.03, 0.04]	0.09 [0.09, 0.10]	0.15 [0.14, 0.16]	0.26 [0.24, 0.28]

Table 8: Results (mean $\pm$ CI) for $\{0\%, 10\%, 25\%\}$ expert error rates in the dataset, with different model combinations.

Takeaway: Our method shows mixed robustness to noisy expert demonstrations: some policy–discriminator pairs degrade sharply beyond 10% corruption, while others (notably Qwen-2.5-7B and Llama3.1-3B) remain competitive or even improve with 25% corrupted expert traces, indicating partial robustness.

D.8 Transferring Pretrained Reward Discriminators

In this section, we are interested in observing the effect of the algorithm being only on-policy. This means we analyse how well a trained reward discriminator transfers to a new policy model. In Table 9 we observe that, across all four combinations C1–C4, reusing a pretrained discriminator and keeping it fixed leads to a substantial drop in pass@k performance compared to the corresponding AIRL run where policy and discriminator are trained jointly from scratch (with C2 almost collapsing, achieving near-zero pass@1). The training curves in Figures 30–33 show a consistent pattern: when a new policy is trained against a frozen discriminator, reward and correctness initially increase during the first 50–100 optimisation steps, but then both training and evaluation rewards, as well as correctness accuracy, deteriorate as training progresses. Since this decline occurs on both training and evaluation metrics, it is not well explained by classical overfitting; instead, it suggests that the discriminator quickly becomes misaligned with factual correctness once the policy moves away from the trajectory distribution on which the discriminator was trained. These results indicate that our reward discriminators are strongly specialised to the reasoning model they are co-trained with and do not reliably transfer to new policies, so in practice our approach behaves as effectively on-policy and benefits from joint updates of policy and discriminator.

ID	Policy (P)	Discriminator (D)	pass@1	pass@3	pass@5	pass@10
C1	Qwen-2.5-3B-Instruct	Qwen-2.5-0.5B-Instruct	**0.51** [0.49, 0.53]	**0.72** [0.71, 0.74]	**0.80** [0.78, 0.81]	**0.87** [0.85, 0.88]
	Qwen-2.5-3B-Instruct	pretrained D from C3	0.29 [0.28, 0.31]	0.49 [0.47, 0.51]	0.57 [0.55, 0.60]	0.67 [0.64, 0.69]
C2	Llama3.2-3B-Instruct	Llama3.2-1B-Instruct	**0.32** [0.30, 0.33]	**0.53** [0.51, 0.55]	**0.63** [0.61, 0.65]	**0.75** [0.73, 0.77]
	Llama3.2-3B-Instruct	pretrained D from C4	0.01 [0.01, 0.01]	0.03 [0.03, 0.04]	0.05 [0.04, 0.06]	0.10 [0.08, 0.11]
C3	Qwen-2.5-7B-Instruct	Qwen-2.5-1.5B-Instruct	**0.71** [0.69, 0.73]	**0.88** [0.87, 0.90]	**0.92** [0.91, 0.93]	**0.95** [0.94, 0.96]
	Qwen-2.5-7B-Instruct	pretrained D from C1	0.10 [0.09, 0.11]	0.25 [0.24, 0.26]	0.35 [0.34, 0.37]	0.52 [0.50, 0.55]
C4	Llama3.1-8B-Instruct	Llama3.2-1B-Instruct	**0.49** [0.47, 0.51]	**0.73** [0.71, 0.75]	**0.80** [0.79, 0.82]	**0.88** [0.86, 0.89]
	Llama3.1-8B-Instruct	pretrained D from C2	0.26 [0.25, 0.28]	0.52 [0.50, 0.54]	0.64 [0.62, 0.66]	0.77 [0.75, 0.79]

Table 9: Each combination ID C1–C4 denotes a pair of policy (P) and discriminator (D) models. AIRL rows train both models jointly from scratch. Transfer rows reuse the discriminator pretrained in the corresponding AIRL combination, keeping D fixed while training P.

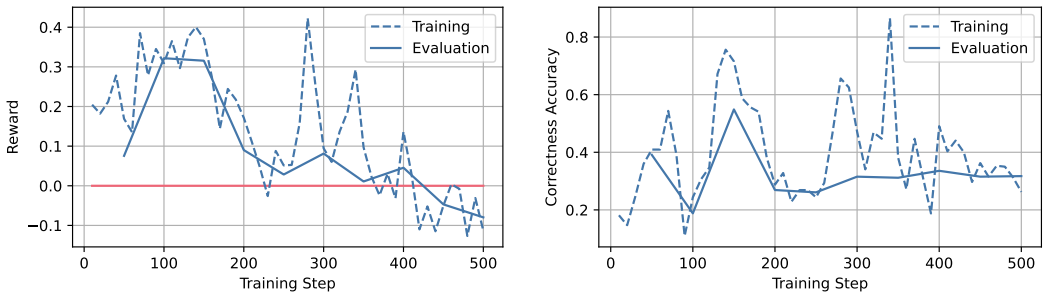

(a) Learned Rewards (b) Correctness Accuracy

Figure 30: **Training behaviour of the Reward and Correctness.** Subfigure 30a shows the training and evaluation reward during optimisation, and Subfigure 30b demonstrates the increasing correctness for the (`Qwen2.5-3B-Instruct - Qwen2.5-0.5B-Instruct`) combination.

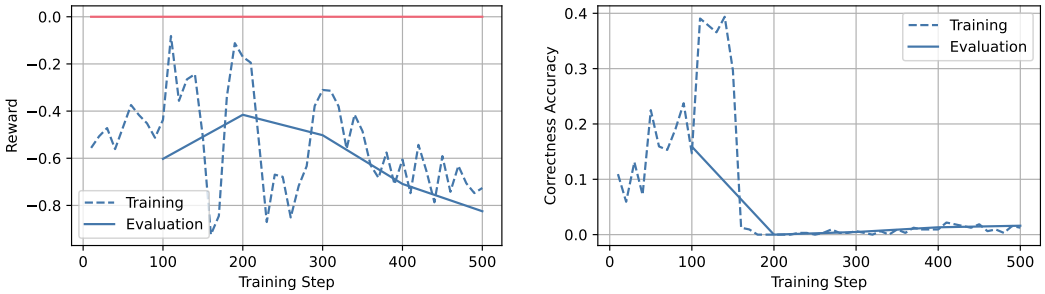

(a) Learned Rewards (b) Correctness Accuracy

Figure 31: **Training behaviour of the Reward and Correctness.** Subfigure 31a shows the training and evaluation reward during optimisation, and Subfigure 31b demonstrates the increasing correctness for the (`Llama3.1-3B-Instruct - Llama3.2-1B-Instruct`) combination.

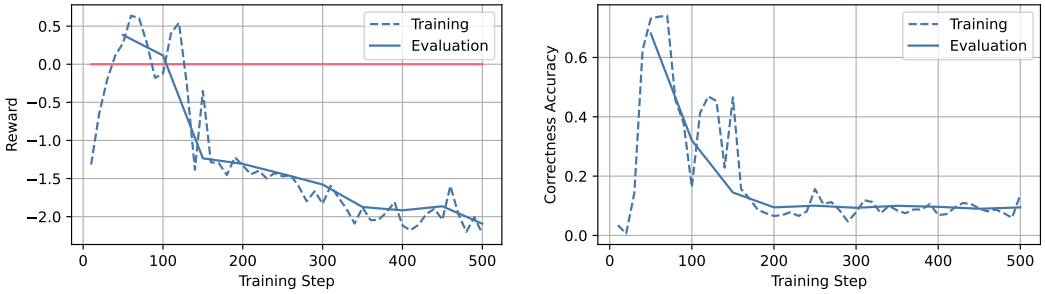

(a) Learned Rewards (b) Correctness Accuracy

Figure 32: **Training behaviour of the Reward and Correctness.** Subfigure 32a shows the training and evaluation reward during optimisation, and Subfigure 32b demonstrates the increasing correctness for the (`Qwen2.5-7B-Instruct - Qwen2.5-1.5B-Instruct`) combination.

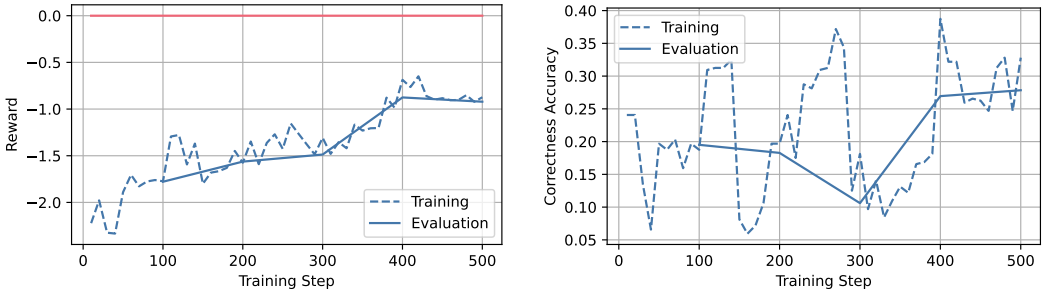

(a) Learned Rewards (b) Correctness Accuracy

Figure 33: **Training behaviour of the Reward and Correctness.** Subfigure 33a shows the training and evaluation reward during optimisation, and Subfigure 33b demonstrates the increasing correctness for the (`Llama3.1-3B-Instruct - Llama3.2-1B-Instruct`) combination.

Takeaway: Reward discriminators trained in our AIRL setup specialise to the policy they are co-trained with and transfer poorly to new policies; when the discriminator is frozen, pass@k performance and correctness accuracy degrade over training, indicating that our method is effectively on-policy and that reliable use requires joint training of policy and discriminator.

D.9 RERANKING WITH HEURISTICS

In this experiment, we are interested in reranking at test-time with heuristics, such as the length of the reasoning response. Therefore, we rank the response according to the longest chain-of-thought and report our results in Figure 34. We observe that the dense reasoning model still outperforms this heuristic reranking approach.

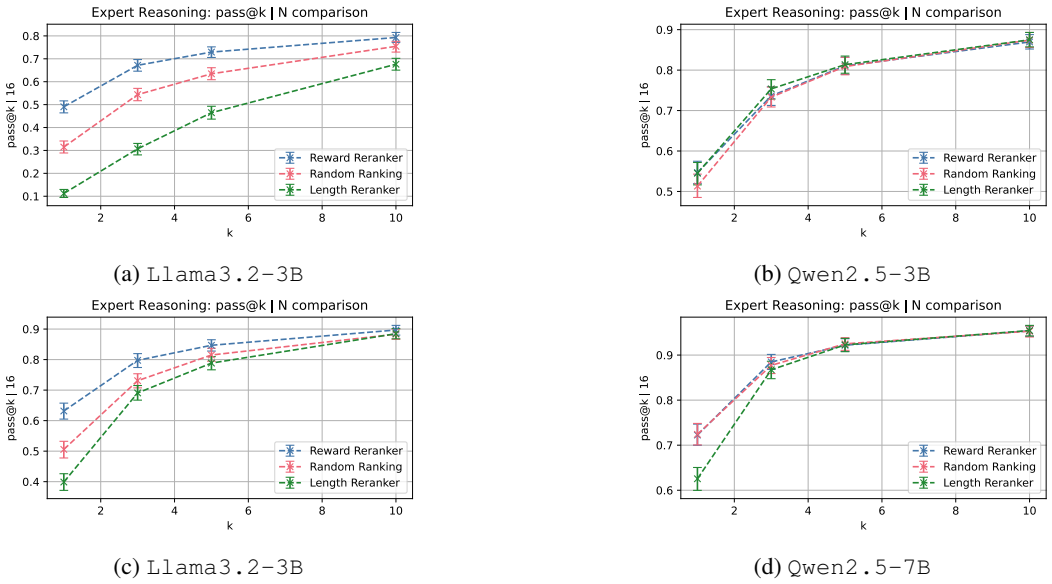

(a) `Llama3.2-3B` (b) `Qwen2.5-3B`

(c) `Llama3.2-3B` (d) `Qwen2.5-7B`

Figure 34: **Reranking at Test-Time with Length Heuristic.** We test the performance of the models, based on re-ranking with the length of the responses. Longer responses are ranked higher than shorter ones.